Reply to Reviewer Comments

(C and R denotes comment and reply, respectively)

Reviewer 1:

General comments:

C1: The manuscript presents an analysis of three debris flow events in China using seismic signals, camera footage and post-events field work. As I understand it, this work could be a significant contribution to debris flow monitoring techniques, by analysing how one or two seismic stations can be used to estimate in real time the velocity and scale of debris flow events. In this perspective, the manuscript is interesting. However, there are major shortcomings that first need to be addressed, regarding in particular the validation of the methodology, the interpretation of the data, the quantitative description of the events (the results are often only qualitative) and the quality of the manuscript (redaction and figures). More generally, I think what is presented in the abstract as a "theoretical basis (…) for the reconstruction of the debris flow process" corresponds more, in the present form of the manuscript, to an application to a case study. A more robust, quantitative and systematic method should be presented to "offer a framework for upscaling debris flow monitoring networks". Here it is not clear what the manuscript first objective is: improving real-time monitoring techniques or improving post-event characterization techniques?

Besides, the contribution of this work to current research, and its innovative aspect in comparison to previous studies cited in the introduction that also analyse debris flows with seismic signals, are not clear to me.

R1: Thank you for the professional and pertinent advice on the manuscript structure and key point of this manuscript. After changing structure of the manuscript, we cannot achieve the validation of the methodology, the interpretation of the data, the quantitative description of the events. The quality of the manuscript (redaction and figures) has been improved.

After carefully analyzing the constructive guidance given by the reviewer regarding the manuscript's innovations, objective, etc., we determined the innovations of this study "a theoretical basis and a case study exemplar for the real-time monitoring, analyzing the debris flow by a debris flow monitoring system based on the core of seismic monitoring, offering a framework for extreme environment upscaling debris flow monitoring networks, the determination of early warning thresholds and hazard assessment and analysis".

Debris flow usually occurs in the area where there is dangerous terrain and poor transportation, and it is difficult to set up many large instruments at the ideal site for continuous monitoring. In addition, it doesn't usually have electric power and the instruments need battery to offer electric power which is lacking in the uninhabited

area. Solar energy can be usually considered to solve the problem of lack of electric power in mountainous areas. However, there is lack of enough sunlight to offer enough solar energy to support monitoring debris flow with instruments of high electric power consumption.

Our study aims to offer a low-cost, reliable, convenient method to establish a debris flow monitoring system based on the core of seismic monitoring. Thus, we use infrared cameras with 5-min interval shoots characterized by less power consumption instead of video equipment. The main advantages of the seismic monitoring are long-distance, remote monitoring and rich information on event dynamics. Our research can offer a case for other researchers to monitor debris flow in similar areas.

Based on this point, the abstract part of the manuscript was rewritten, which focuses more on a detailed description of the results obtained from the technical line of this research and highlights more the advantages of this research. The revised abstract is as follows:

Lines 25 to 51

Debris flows triggered by rainfall are among the world's most dangerous natural hazards due to their abrupt onset, rapid movement, and large boulder loads that can cause significant loss of life and infrastructure. An important approach to mitigating debris flows is monitoring and early warning. However, it is difficult to deploy many large instruments in an ideal location for continuous monitoring due to complex topographic condition of areas like Wenchuan, China. In addition, there is usually no electricity, and it is difficult to place more batteries to provide power for the large instruments, which is unavailable in the area with dangerous terrain and poor transportation. Given that environmental seismology has proven to be a powerful method for monitoring debris flows and other geohazards, our study aims to establish a debris flow monitoring system based on the core of seismic monitoring which is proven to be cost-effective, reliable, practical, and monitored three debris flows of different scale in Wenchuan, China. We comprehensively analyzed seismic signals and infrared images gained by the system with other post-event field investigations to obtain basic parameters such as debris flow velocity and grain size. First, we selected the second debris flow in the Fotangbagou gully as a case to show the process to determine the duration of the debris flow that passed the monitoring station by the energy recovered seismic signal, and establish that rainfall triggered the debris flow. Second, we comprehensively analyzed the infrared imagery, the power spectral density (PSD) and the PSD forward, and revealed that the debris flow seismic energy and its frequency spectrum characteristic are highly correlated with the development process of the debris flow; and the three debris flows were analyzed to show the seismic characteristics of rapid excitation and slow decay. Finally, the cross-correlation function is used to calculate the maximum velocity of 7.0 m/s of the second debris flow, which was confirmed by the Manning formula. The study

provides a theoretical basis and a case study example for real-time monitoring, analysis of a debris flow monitoring system based on seismic signal, early warning, and hazard assessment.

C2: Definition of the quantified characteristics of the debris flow that will be estimated from seismic signals: velocity, discharge, sediment concentration and granulometry, …

R2: Thank you for your constructive comments. Obtaining quantified characteristics of the debris flow from seismic signal is the ultimate goal of debris flow seismology, and some researchers have tried to reconstruct the dynamical parameters of the debris flow from the low-frequency information of the large-scale debris flow seismic data observed in the far-field. However, the low-frequency information in the seismic data observed in the near-field is weak (only ultra-large scale debris flow has relatively high quality low frequency signal), and the high-frequency information is too complicated for the inversion to obtain the quantified characteristics of the debris flow. In this research, we still aim to semi-quantitative characteristics analysis of debris flow about its velocity, discharge, sediment concentration and granulometry estimated from seismic signals. We agree with the reviewer, and the quantified analysis is our next research purpose.

The part about velocity, discharge, sediment concentration has been modified in the section “Infrared imagery analysis”, as follows:

Lines 494 to 575

The analysis of a series of infrared images of debris flows serves as a reliable method for validating the accuracy of the process reconstruction performed through debris flow seismic studies. Infrared imaging, particularly during nighttime conditions, often presents challenges due to its limited visible range and lower resolution. Consequently, the first Fotangbagou debris flow and the Ergou debris flow, both of which occurred at night, suffered from suboptimal image quality, making them less suitable for analysis. To address these limitations, we opted to focus our verification analysis on the second debris flow in Fotangbagou Gully, which occurred during daytime conditions. This choice allowed us to benefit from improved image quality and clarity, making it a more suitable example for our analysis.

Infrared images were captured at 5-minute intervals between 7:39 and 8:04 (Fig. 7b-7g) during the debris flow event. However, the image quality suffered due to water droplets on the camera lens caused by the passage of the debris flow, resulting in blurry images at station 2. Consequently, we chose to rely solely on the infrared camera at station 1 for our analysis. The early infrared images (Fig. 7b-7g) illustrate a gradual increase in both discharge and particle content of the debris flow, with a peak occurring around 7:54. However, the changes in velocity appeared to exhibit

complexity during this phase. In contrast, the later images (Fig. 7e-7g) depict a reduction in particle content, a decrease in flow rate, and lower velocities, with distinct flow characteristics evident towards the end (Fig. 7g). The overall trend in debris flow evolution, as observed through infrared imagery, aligns with the trend observed through seismic analysis. In a macroscopic perspective, seismic signals effectively capture the general development trend of the debris flow. However, it's noteworthy that the peak state time of the debris flow, as indicated by the infrared imagery, does not coincide with the seismic data. To comprehensively analyze this discrepancy, we will delve into a detailed examination of the dynamic features of the debris flow, including discharge, flow velocity, and particle content, as reflected in the imagery. Additionally, in the next section, we will combine this analysis with the PSD forward modeling to gain further insights.

At 7:39 (Fig. 7b), the discharge of the debris flow remained relatively low. At this point, point A, located at a higher position within the old channel, remained unaffected by inundation. Most of the flow was concentrated along its right channel, with only a small portion following the left channel. There was no evidence of flooding or erosion along the left bank at point B. By 7:44, the debris flow initiated the flooding of point A and began eroding the left bank at point B. The water depth and left bank erosion reached their maximum extent in the image captured at 7:59. Subsequently, the water depth began to decrease. In summary, the infrared imagery reveals a gradual increase in flow rate between 7:39 and 7:54, followed by a gradual decrease after 7:54.

Regarding particle content, it follows a similar trend to the discharge. Specifically, there is a gradual increase in particle content from 7:39 to 7:49. This elevated particle content is sustained between 7:49 and 7:54, after which there is a notable decrease in particle concentrations observed at 7:59 and 8:04.

Regarding flow velocity, it exhibited an interesting pattern, with its highest point observed at 7:39, followed by a gradual decrease as observed at point C, where it remained relatively stable across the six consecutive infrared images. At this location, marked as point C, the flow exhibited maximum turbulence in Fig. 7b, indicating peak velocity, which then gradually declined. In Fig. 7d and 7e, eddies are visible near point A, situated at a higher position, suggesting the possibility of higher flow velocities at both moments. Conversely, the flow pattern at point C, upstream, indicated relatively slower velocities at both instances. Eddies near point C could be attributed to excessive discharge originating from lower elevations.

Analyzing the evolution of the debris flow, we observed a gradual increase in debris flow discharge from 7:39 to 7:59. This increase can be attributed to the relatively high flow velocity during this period, leading to intensified erosion along the course of the rock and soil body adjacent to the accumulation area. As a result, the

fluid-solid phase material content increased, leading to a tendency for the flow rate to rise. At 7:59, the flow velocity decreased to some extent, resulting in weaker erosion. The debris flow gradually transitioned into a state resembling a “flood”. In Fig. 7f, point A exhibits a stationary stone block that cannot be moved, and in Fig. 7g, the rock bed becomes clearly visible. These observations indicate that the erosion capability and carrying capacity of the debris flow were weak at this moment. This complex behavior in the trend of flow velocity, discharge, and particle composition changes during the debris flow’s evolution underscores the inconsistency in their characteristics. In the next section, we will integrate these variables with the seismic PSD forward modeling of debris flow generation to analyze their respective impacts on the signal. This analysis will provide insights into the contradictory peak time observations between infrared imagery and seismic interpretation.

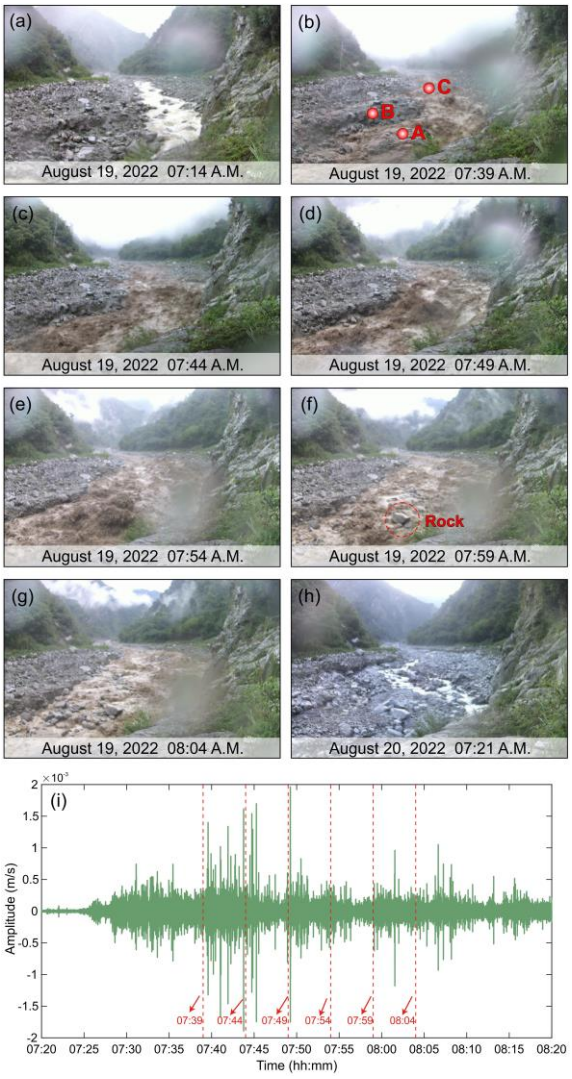

Fig. 7. Infrared camera images and seismic signals were recorded at monitoring point 1 in Fotangbagou Gully during the second debris flow on the morning of August 19, 2022. Images (b)-(g) were recorded every 5 minutes from 7:39 to 8:04: (a) before debris flow; (b) 7:39 frame; (c) 7:44 frame; (d) 7:49 frame; (e) 7:54 frame; (f) 7:59

frame; (g) 8:04 frame; (h) after debris flow. (i) The seismic signal was recorded at the point.

The infrared images show a gradual increase in the particle content of the debris flow from 7:39 to 7:49, with high particle content maintained between 7:49 and 7:54 but far lower concentrations at 7:59 and 8:04. The debris flow evolution analysis showed flow velocity increased gradually from 7:39 to 7:59, and was relatively high; in this condition, there is intense erosion of accumulations next to the channel and entrainment along the flow path, which increases the proportion of solid phase in the fluid. As flow velocity decreases, erosion weakens and the particle content gradually decreases, turning the debris flow into a water flood. The presence of a rock at point A in Fig. 7f and 7g illustrates the lack of transport capacity at this stage of the debris flow.

The part about velocity has been modified in the section “Debris flow velocity analysis”, as follows:

Lines 742 to 772

The time domain signal was used to solve the mean velocity of each debris flow between the two monitoring stations using the cross-correlation function (Eq. (4)). The velocity result of 38.3 m/s for Ergou gully is an order of magnitude higher than 3.0 m/s and 7.0 m/s for Fotangbagou gully and is outside the normal debris flow range (Table 3) which indicates the order of magnitude is 1 (Arattano and Marchi, 2005; Cui et al., 2018). The signal lag time τ in Eq. (4) reflected by the peak amplitude of the second debris flow in Fotangbagou gully is 74 s (Fig. 11), and the distance between adjacent monitoring sections is about 520 m, which gives a mean velocity of 7.0 m/s (Table 3). For the first debris flow of Fotangbagou and the debris flow of Ergou, τ are 173 s and 12 s, mean velocities are 3.0 m/s and 38.3 m/s. Since the nighttime infrared images could not be used, R could only be determined for the second debris flow in the Fotangbagou gully, which took place in daylight.

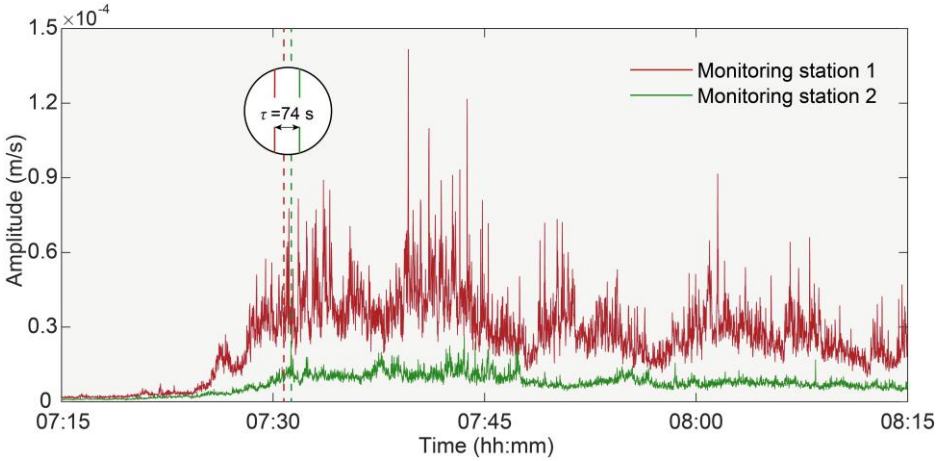

Fig. 11. Amplitude range (vertical direction) of the second debris flow in Fotangbagou gully based on the cross-correlation function. The signal lag time τ between the two monitoring stations is circled.

Table 3 Results of mean velocity calculations for Fotangbagou gully and Ergou gully debris flows.

Debris flow	Mean velocity calculated using each method (m/s)	
	Cross-correlation function	Manning formula
First debris flow in Fotangbagou Gully	3.0	—
Second debris flow in Fotangbagou Gully	7.0	7.9
Debris flow in Ergou Gully	38.3	—

Notation: Since the nighttime infrared images could not be used, *R* could only be determined for the second debris flow in the Fotangbagou gully, which took place in daylight.

The Manning formula has its own uncertainties indeed, but Cui et al. (2013), Guo et al. (2016), and Cui et al. (2018) thought it is effective to use this formula to estimate the velocity of debris flows. Using the Manning formula on this only event, the maximum debris flow velocity at monitoring points 1 and 2 was calculated as 7.8 and 7.9 m/s, respectively. It indicates that the values of velocities are constant during process between the stations 1 and 2 because of the comparative wide and straight channel possibly. This indicates it is appropriate to use the cross-correlation function to estimate the velocity of debris flow because the two values from cross-correlation and from the Manning formula have a smaller difference.

Reference

Arattano, M., Marchi, L., 2005. Measurements of debris flow velocity through cross-correlation of instrumentation data. Nat. Hazards Earth Syst. Sci. 5(1), 137-142.

Cui, P., Guo, X., Yan, Y., Li, Y., Ge, Y., 2018. Real-time observation of an active debris flow watershed in the Wenchuan Earthquake area. Geomorphology 321, 153-166.

Cui, P., Zhou, G.G., Zhu, X.H., Zhang, J.Q., 2013. Scale amplification of natural debris flows caused by cascading landslide dam failures. Geomorphology 182, 173-189.

Guo, X., Cui, P., Li, Y., Zou, Q., Kong, Y., 2016. The formation and development of debris flows in large watersheds after the 2008 Wenchuan Earthquake. Landslides 13, 25-37.

C3: Explanation of how these characteristics are estimated from seismic signals (if I get it correctly, estimation of the PSD from seismic signals to invert for u (and D) in eq 8 + cross-correlation between two seismic stations)

R3: We totally agree with the reviewer's suggestion. After changing structure of the manuscript, we analyse characteristics of debris flow by combination with infrared imagery, post-event field investigation. Besides, we also cannot directly invert for *u* (and *D*) based on estimation of PSD in Eq. (7) for the near-field seismic is too complicated. Instead, we can only get semi-quantitative characteristics analysis of *u* (and *D*) based on estimation of PSD in Eq. (7), we just use the relation expressed by Eq. (7) to analysis the PSD gained by Eq.(8). We get semi-quantitative analysis of flow velocity between two seismic stations based on cross-correlation function.

Estimation of the PSD from seismic signals to invert for *u* (and *D*) in Eq. (7) is modified, as follows:

Lines 615 to 690

Eq. (6) was employed to calculate the seismic Power Spectral Density (PSD) curves for the six-time points corresponding to the infrared images (Fig. 9a). Notably, the maximum energy within the main frequency band (15~30Hz) exhibited a gradual decline from 7:39 to 8:04, evident from the discernible trend in dot changes depicted in Fig. 9a. The width of the PSD spectrum demonstrated an initial increase, followed by a subsequent decrease, showing distinct trends between the low-frequency and high-frequency bands. Specifically, the high-frequency band (>30Hz) experienced a gradual reduction from 7:39 to 8:04, characterized by a rapid decrease from 7:39 to 7:49 and a relatively slower decline from 7:54 to 8:04. Conversely, the low-frequency band (<15Hz) exhibited a substantial increase from 7:39 to 7:44, followed by a more

substantial decrease leading up to 7:54, after which it roughly remained unchanged. These varying characteristics among different frequency bands underscore the need for a deeper understanding. In the subsequent sections, we will employ a debris flow seismic PSD forward model to gain a more comprehensive insight into these observations.

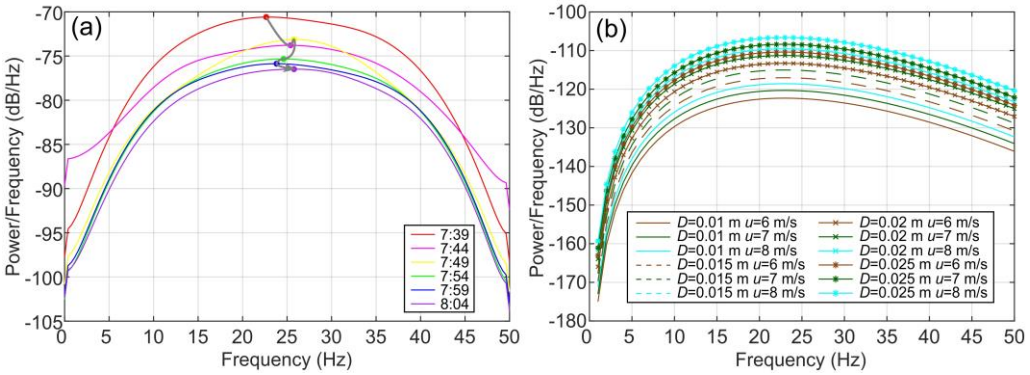

Fig. 9. Characteristic change of power spectral density (PSD). (a) Evolution of PSD during the second debris flow in Fotangbagou Gully on the morning of August 19, 2022, from 7:39 to 8:04; (b) Comparison of PSD for different grain sizes (D) and velocities (u). Each curve represents PSD frequency over 60 s. The six dots in subplot (a) correspond to the PSD maximum at the six-time points from 7:39 to 8:04, and the black arrows indicate the time course of these six-time points. The PSD values of D=0.015 m and u=8 m/s, D=0.02 m and u=6 m/s are equal, so the curves coincide in subplot (b).

We conducted debris flow seismic Power Spectral Density (PSD) forward modeling (Fig. 9b), employing Eq. (7) with key parameters derived from observations of the 2nd debris flow in Fotangbagou. D was determined based on 94% of the particle size, resulting in values of 0.01 m, 0.015 m, 0.02 m, and 0.025 m, respectively. The velocity u was consistent with the mean velocity described in Section 4.3, which was set at 2 m/s, 4 m/s, and 6 m/s. The seismic propagation distance r_0 was determined by measuring the distance between Point 1 and the central channel of the 2nd debris flow in Fotangbagou gully. All other parameters in Eq. (7) remained consistent with those used for seismic signal recovery, as detailed in Section 4.1.

As depicted in Fig. 9b, it is evident that the velocity of the debris flow significantly determines the energy level of the PSD, while the particle size exerts a comparatively weaker impact on energy levels than flow velocity. Specifically, for a debris flow with the same particle radius, the energy across the entire frequency band experiences a sharp increase with higher flow velocities. In contrast, the increase in energy within each specific frequency band remains relatively modest when varying particle size at a consistent flow velocity.

The impact of flow velocity is more pronounced at the high-frequency end compared to the low-frequency end. This suggests that variations in flow velocity can be effectively discerned by analyzing the energy at the high-frequency end of the PSD curve. When examining the PSD curves for the six-time points corresponding to the infrared images, it becomes evident that the high-frequency end of the curve gradually decreases. This decrease signifies a gradual reduction in the debris flow velocity. Notably, the velocity decline is relatively rapid from 7:39 to 7:59 and then exhibits a slower rate of decrease. These observations align with the inferences drawn from the analysis of flow rates based on the infrared imagery.

In the low-frequency range, velocity has a notable impact on energy. When velocity decreases, the energy corresponding to a single frequency also decreases, albeit with a relatively small amplitude compared to the high-frequency range, as illustrated in Fig. 9. Notably, there is an observable increase in the low-frequency end at 7:44 in contrast to 7:39, which contradicts the analysis of the high-frequency range. Fig. 7c displays an infrared image indicating a relatively high concentration of particles within the debris flow at 7:44. This observation suggests that the strong energy observed at the low-frequency end in this timeframe may be attributed to the presence of these particles.

The peak frequency is influenced by both particle size and flow velocity, as demonstrated in Fig. 9b. When examining the relationship between particle size D and flow velocity u, it becomes evident that a smaller particle size and higher flow velocity result in a larger peak frequency in this debris flow, and vice versa. This phenomenon is attributed to the combined effects of particle size and flow velocity. Additionally, it's worth noting that particle content, including flux and concentration, plays a significant role in affecting the energy of seismic signals. Therefore, when considering the model described in Eq. (7), it is imperative to account for the influence of particle concentration. Analyzing the peak frequency of seismic signals from debris flows captured between 7:39 and 8:04, as shown in Fig. 9, reveals an interesting pattern. Initially, the peak frequency increases, then decreases, and eventually rises again. This behavior can be attributed to the comprehensive response of particle size and flow velocity to the PSD. Specifically, when flow velocity decreases, the particle size of debris flows transported by the debris flow increases. It's important to recognize that significant changes in flow velocity should be accompanied by corresponding alterations in sediment concentration.

From our analysis, we conclude that in the six moments from 7:39 to 8:04, the flow velocity gradually decreases and the particle size, particle concentration, and flow velocity first increase and then decrease. This pattern is consistent with the results of the infrared image analysis in Section 4.2.2 and confirms that the trend of the debris flow can be determined from the time-frequency characteristics of the seismic signals.

Cross-correlation between two seismic stations is modified, which is shown in R2 of general comment for reviewer 1 from lines 742 to 772.

C4: Explanation of how the methodology is validated using a specific debris flow event and other data / methods to estimate the debris flow characteristics (camera footage, post-event field work, …)

R4: We deeply appreciate the reviewer carefully went through the manuscript line by line. The fact that the methodology is validated for other debris or not is also an important concern. Thus, we chose seismic of 2nd debris flow in Fotangbagou gully as a case to restore seismic power, identify duration of the debris flow flowing through the monitoring station and determine that rainfall triggered the debris flow. Secondly, we comprehensively analysed monitored imagery of debris flow, the debris flow seismic power spectral density (PSD) and PSD forward, clearly explained strong correlation of seismic power, frequency range characteristic change of and debris flow evolution process. Three debris flows were analysed that they exhibit the seismic characteristics of fast excitation and slow recession. We attempt to address the validity of the present methodology in this context.

The section "Post-event field investigation" is modified to estimate the debris flow characteristics, as follows:

Line 577 to 610

The field investigation and UAV survey at Fotangbagou Gully started on the third day after the debris flow events, and nearby villagers confirmed the accumulation fans had not been disturbed. UAV aerial imagery of the accumulation fan at the gully mouth and close-ups of surface conditions are shown in Fig. 8a–8c. Field measurements indicate the fan is about 1.2 m thick, with a thin layer (1–2 mm) of clay covering the surface in several areas (Fig. 8c). Some rocks with diameter larger than 1 m in Fig. 8b and 8c show that the debris flow has a relatively high carrying capacity, and the rocks at the bottom of the alluvial fan are relatively large (Fig. 8b), while the rocks in the front part of the alluvial fan (Fig. 8c) are relatively small, indicating that the carrying capacity of the debris flow sharply decreases after it is released from the channel constraints (or in other words, the cross-sectional area increases).

A sediment sample was collected from the accumulation fans in the Fotangbagou gully to estimate the particle size distribution of the debris flow. The sample (Fig. 8e) of about 4.7 kg was taken around the location marked ① in Fig. 8a. Grain size analysis was undertaken by sieving and a Malvern particle sizer. Due to lack of several sample analysis in this study, we should consider finishing several sample

analyses to estimate the variability in other researches. We forgot to record the fraction of materials that was above the maximum particle size displayed in the granulometric curve. Thus, we should finish it in other similar researches. The results show that clay, i.e., particles with grain size less than 0.005 mm, accounted for only 0.041% of the total weight of the sample from the channel (Fig. 8d), which is consistent with field observations. The low cohesive sediment content of the accumulation fan sample could be due to removal by post-event processes, either by the flushing action of the Minjiang River or by human clearance of the impoundment fan. The particle size distribution shows that 94% of the particle size of the sample is 0.018 m, i.e., D in Eq. (7). In the next section, we will use D as a guide for forward analysis of the PSD curve features of the debris flow.

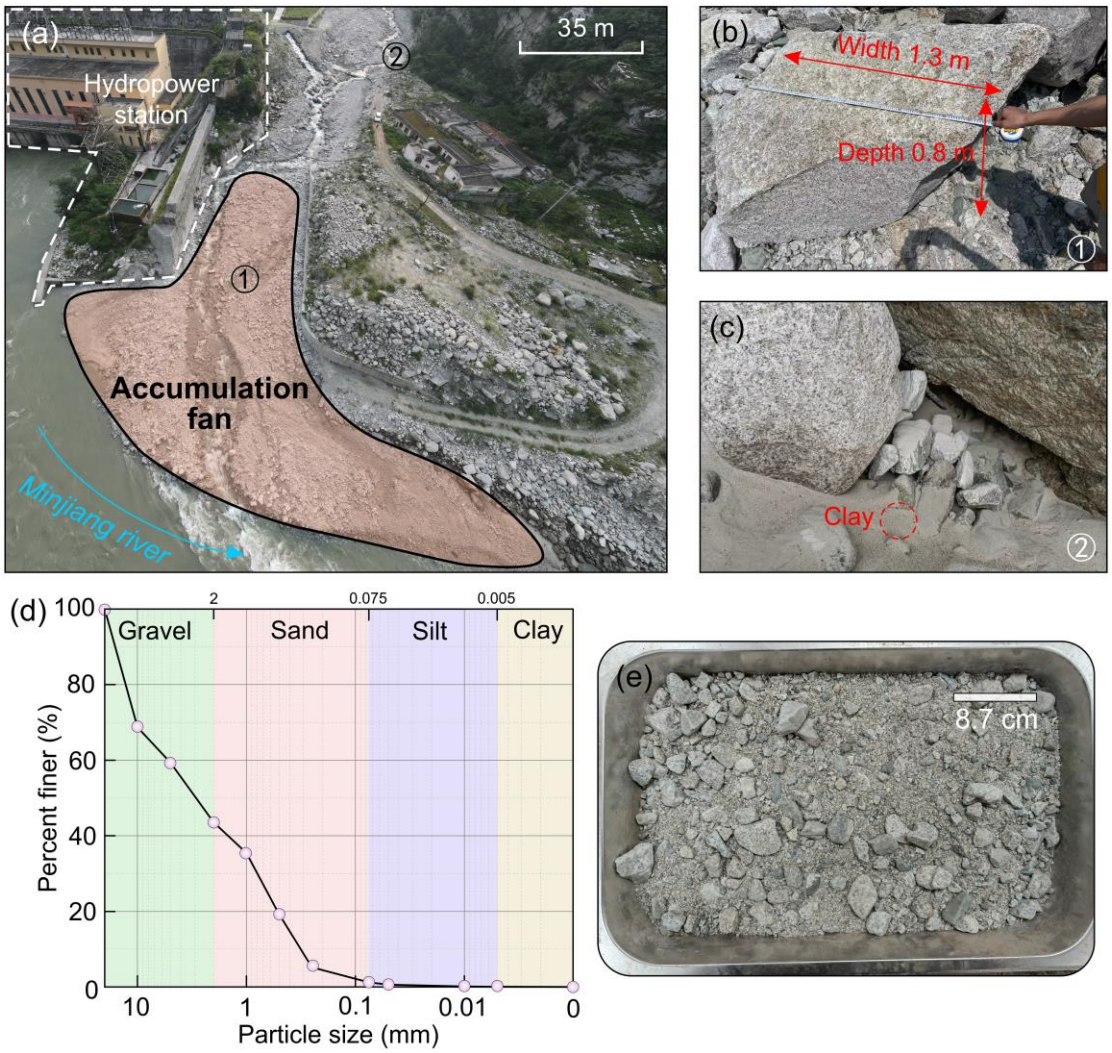

Fig. 8. Post-event field survey of accumulation fans in Fotangbagou Gully. (a) Aerial view of the Fotangbagou gully fan; (b) Largest particle on the Fotangbagou gully fan, marked ① in image (a); (c) Thin layer of clay covering the accumulation surface in Fotangbagou gully, marked as ② in image (a); (d) Particle size distribution for Fotangbagou gully sediment samples; (e) Fotangbagou gully sediment sample. Clay

has not been marked in the subplot (d) because the particles with grain size less than 0.005 mm account for 0.041% of the total weight of the sample.

The section "Infrared imagery analysis" is modified to estimate the debris flow characteristics, which is shown in R2 of general comment for reviewer 1 from lines 494 to 575.

C5: Application of the method to two other debris flows.

R5: Thanks a lot for the constructive comment. In this study, we take the 2nd Fotangbagou gully debris flow as an example to discuss the feasibility of our methodology and research ideas. Just as the two other debris flows are relatively lack of information, at the same time, and analysing the two other debris flows just like the 2nd Fotangbagou gully debris flow will make the manuscript appear redundant. This study mainly uses seismic signals to analyse the whole evolution process of debris flows.

We have modified application of the method to two other debris flows in section "Reconstruction of 1st Fotangbagou and Ergou debris flow process", as follows:

Lines 692 to 740

The seismic signal restoration was then completed using the same parameter values as the first debris flow in Section 4.1 for the first Fotangbagou debris flow. The horizontal distances, representing the separation between the channel and the monitoring station in the horizontal direction for Ergou Gully, are 13 m and 7 m for monitoring points 1 and 2, respectively. For the Ergou debris flow restoration, a gain factor of 1.8 (i.e., *Q* in Eq. (8)) was used at monitoring station 1, and the parameter values for monitoring stations 2 and 1 of Fotangbagou were used for Ergou monitoring stations 1 and 2.

Seismic signal data for monitoring points 1 and 2 in Fotangbagou Gully are shown in Fig. 10a to 10d. The first debris flow passed monitoring point 1 at about 3:07, after which debris flow movement gradually strengthened until 3:13 when the signal amplitude peaked and slowly declined thereafter. After the debris flow passed monitoring point 2 around 3:10, there were about 120 s of rapid vibration, amplitude peaked, then the seismic signal began to weaken. After about 160 s, debris flow movement gradually strengthened to a second amplitude peak at 3:24 and then decayed slowly. The seismic signal was stronger at monitoring point 1 than at point 2, and there was a general decrease in energy generated by the movement of the debris flow between the two points. The time-frequency characteristics of the seismic signal at monitoring point 1 (Fig. 10b) reveal a concentration of high-energy components, indicated by red or dull-red colors in the color bar, within the 12–44 Hz range from

3:07 to 4:25. Over the entire duration of the event, there is a gradual decay in high-energy components towards 21 Hz. At monitoring point 2 (Fig. 10d), the high-energy components, represented by red or dull-red colors in the color bar, are concentrated within the 10–42 Hz range from 3:10 to 4:00. Over the entire duration of the event, the high-energy components gradually decrease, with the red or dull-red colors indicating decay towards 21 Hz. At both monitoring points, the spectrogram shows the same pattern of rapid rise and slow decline of the amplitude seismic signal in the time domain.

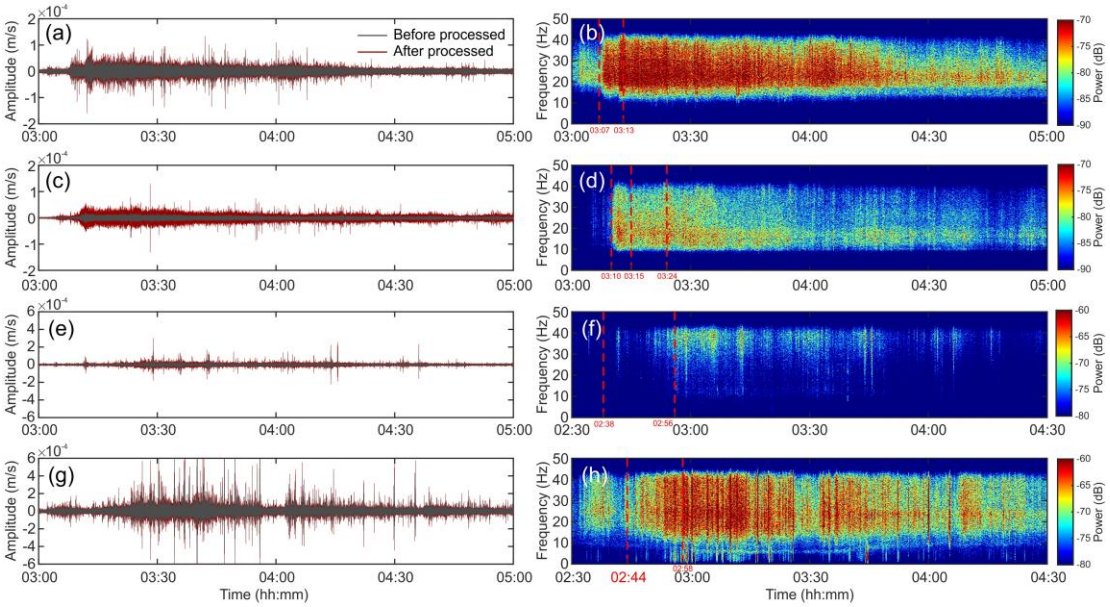

Fig. 10. seismic and its spectrogram of the first debris flow in Fotangbagou gully and debris flow in Ergou gully. The first Fotangbagou debris flow's Seismic recorded at monitoring stations 1 (a) and station 2 (c), and (b) and (d) is its spectrogram respectively; The Ergou debris flow's Seismic recorded at monitoring station 1 (e) and station 2 (g), and (f) and (h) is its spectrogram respectively.

Seismic signal data for the two monitoring points in Ergou Gully are shown in Fig. 10e to 10h. As the debris flow passed monitoring point 1 at about 2:38, it was moving rapidly and strongly; signal amplitude peaked at 2:56 and then decayed slowly. The debris flow passed monitoring point 2 at about 2:44, with signal amplitude peaking at 2:58 and slowly decaying. In contrast to Fotangbagou Gully, the seismic signal was stronger at monitoring point 2 than at monitoring point 1, and the energy generated by the movement of the debris flow increased between the two monitoring points. The time-frequency characteristics of the seismic signal at monitoring point 1 show energy is concentrated in the 30–40 Hz range between 2:50–4:00 (Fig. 10f). At monitoring point 2, energy is concentrated in the 6–45 Hz range between 2:45–4:30 (Fig. 10h). Throughout the entire event, there is a gradual energy

decay towards 23 Hz, representing the dominant frequency range with high power, indicated by red or dull-red colors in the color bar, observed at the conclusion of the debris flow in Ergou. As with the Fotangbagou debris flow, the overall trend of the spectrogram is consistent with the amplitude range in the time domain, with a rapid rise and a slow decline.

C6: A detailed review of the paper is also needed to improve the quality of writing and disambiguate some sentences.

R6: Thank you for the helpful comment. We have improved the quality of writing and disambiguate some sentences in the whole manuscript.

Specific comments:

C1: l.26: I am not sure debris flows systematically start abruptly, can't they be initiated by the progressive remobilization of materials by rain water? It is true that their front can be a massive surge, but this is different from the initiation process. Similarly, debris flows do not necessarily transport large boulders, in particular if there are not large boulders in the gully that can be transported.

R1: Thanks a lot for the constructive comment and agree with the reviewer's suggestion. Iverson (1997) proposed debris flows triggered by rainfall can occur with little warning and vary from quiescently streaming, sand-rich slurries to tumultuous surges of boulders and mud, which indicates debris flows can start abruptly and transport large boulders.

It can be modified, as follows:

Lines 25 to 27

Debris flows triggered by rainfall are among the world's most dangerous natural hazards due to their abrupt onset, rapid movement, and large boulder loads that can cause significant loss of life and infrastructure.

References:

Iverson, R.M., 1997. The physics of debris flows. Rev. Geophys. 35(3), 245-296.

C2: l.27-28: monitoring and early-warning systems can mitigate risks associated to debris flows, but can hardly prevent them.

R2: We totally agree with the reviewer's suggestion. We acknowledge preventing risk is achieved difficultly. Thus, we deleted "preventing" and left only "mitigating". It has been modified, as follows:

Lines 27 to 28

An important approach to mitigating debris flows is monitoring and early warning.

C3: l.31-33: In this sentence it is not clear if you want to focus on "combining debris flow imagery with seismic signal analysis" and "post-disaster surveys" to better understand the dynamics of the debris flow once it as occurred, or if you want to focus on the "inversion of seismic signals into dynamic parameters". As I see it, you objective is the second point, and the first point is a mean to achieve the "inversion of seismic signals". You should make it clearer.

R3: Thank you for your helpful comments. We have deleted "inversion of seismic signals into dynamic parameters". Our objective in the abstract has been modified, as follows:

Lines 33 to 36

Given that environmental seismology has proven to be a powerful method for monitoring debris flows and other geohazards, our study aims to establish a debris flow monitoring system based on the core of seismic monitoring which is proven to be cost-effective, reliable, practical, and monitored three debris flows of different scale in Wenchuan, China.

C4: l.50: At this point the reader wonders why you give a velocity estimation for only one debris flow, and not the other two. Besides, why do you give this value and not the velocities estimated with the PSD?

R4: Thank you for your constructive suggestions sincerely. For the first question, there is an error because velocity estimations for the other two debris flow are different from results of Manning's formula, the results of other two event can be proved they are correct difficultly. For the second question, it is difficult to get the velocities estimated with the PSD because there is more than a variable like D, u and so on. Thus, it has been modified, as follows:

Lines 47 to 49

Finally, the cross-correlation function is used to calculate the maximum velocity of 7.0 m/s of the second debris flow, which was confirmed by the Manning formula.

C5: In the introduction you focus on seismic instrumentation but you should also present other monitoring techniques (infrasound, radars, LIDAR, force/strain/pressure sensors, …) and explain why seismic monitoring is complementary. For example:

- *Marchetti, E. et al., 2019. Infrasound Array Analysis of Debris Flow Activity and Implication for Early Warning. Journal of Geophysical Research: Earth Surface 124, 567–587. doi.org/10.1029/2018JF004785 (you refer to this paper when you speak of seismic monitoring, but it actually focuses on infrasound sensors monitoring).*
- *Aaron, J. et al., 2023. High-Frequency 3D LiDAR Measurements of a Debris Flow: A Novel Method to Investigate the Dynamics of Full-Scale Events in the Field. Geophysical Research Letters 50, e2022GL102373. doi.org/10.1029/2022GL102373*
- *Nagl, G. et al., 2020. Velocity profiles and basal stresses in natural debris flows. Earth Surface Processes and Landforms 45, 1764–1776. doi.org/10.1002/esp.4844*
- *Hürlimann, M. et al., 2003. Field and monitoring data of debris-flow events in the Swiss Alps. Can. Geotech. J. 40, 161–175. doi.org/10.1139/t02-087 (you cite this article already, but you can use it to review different monitoring techniques)*

R5: Thanks a lot for the constructive comment. Some sentences have been added or modified, as follows:

Lines 92 to 94

Flow depth and velocity can be effectively measured using radar and ultrasonic instruments (Arattano and Moia, 1999; Kogelnig et al., 2014).

Lines 100 to 103

In a study of a channel at Illgraben in the Swiss Alps, Hürlimann et al. (2003) showed three debris flows had different properties, such as flow depth, flow velocity, and peak flow, and highlighted the effectiveness of ultrasonic and radar devices in monitoring these debris flows.

Lines 105 to 110

Currently, a diverse array of instruments, including infrasound sensors (Marchetti et al., 2019), LiDAR (Aaron et al., 2023), fiber optic sensors (Schenato and Pasuto, 2021; Huang et al., 2012), pressure sensors (Berti et al., 2000; Kean et al., 2012), and normal or shear stress sensors (McArdell et al., 2007; McCoy et al., 2010; Nagl and Hübl, 2017), is being increasingly utilized. These devices are adept at capturing an extensive range of parameters, such as infrasound signal amplitudes, velocities of surfaces and fronts, pressure, stress, among others.

References:

Aaron, J., Spielmann, R., McArdell, B. W., Graf, C., 2023. High-Frequency 3D LiDAR Measurements of a Debris Flow: A Novel Method to Investigate the

Dynamics of Full-Scale Events in the Field. Geophys. Res. Lett. 50(5), e2022GL102373.

Arattano, M., Marchi, L., 2008. Systems and sensors for debris-flow monitoring and warning. Sensors 8(4), 2436-2452.

Arattano, M., Moia, F.,1999. Monitoring the propagation of a debris flow along a torrent. Hydrol. Sci. J. 44(5), 811-823.

Berti, M., Genevois, R., LaHusen, R., Simoni, A., Tecca, P.R., 2000. Debris flow monitoring in the Acquabona watershed on the Dolomites (Italian Alps). Physics and Chemistry of the Earth, Part B: Hydrology, Oceans and Atmosphere 25(9), 707-715.

Huang, C. J., Chu, C. R., Tien, T. M., Yin, H. Y., Chen, P. S., 2012. Calibration and deployment of a fiber-optic sensing system for monitoring debris flows. Sensors 12(5), 5835-5849.

Hürlimann, M., Rickenmann, D., Graf, C., 2003. Field and monitoring data of debris-flow events in the Swiss Alps. Can. Geotech. J. 40(1), 161-175.

Kean, J. W., Staley, D. M., Leeper, R. J., Schmidt, K. M., Gartner, J. E., 2012. A low-cost method to measure the timing of postfire flash floods and debris flows relative to rainfall. Water Resour. Res. 48(5), W05516.

Kogelnig, A., Hübl, J., Suriñach, E., Vilajosana, I., McArdell, B.W., 2014. Infrasound produced by debris flow: propagation and frequency content evolution. Nat. Hazards 70, 1713-1733.

Marchetti, E., Walter, F., Barfucci, G., Genco, R., Wenner, M., Ripepe, M., McArdell, B., Price, C., 2019. Infrasound array analysis of debris flow activity and implication for early warning. J. Geophys. Res.-Earth Surf. 124(2), 567-587.

McArdell, B. W., Bartelt, P., Kowalski, J., 2007. Field observations of basal forces and fluid pore pressure in a debris flow. Geophys. Res. Lett. 34(7), L07406.

McCoy, S. W., Kean, J. W., Coe, J. A., Staley, D. M., Wasklewicz, T. A., Tucker, G. E., 2010. Evolution of a natural debris flow: In situ measurements of flow dynamics, video imagery, and terrestrial laser scanning. Geology 38(8), 735-738.

Nagl, G., Hübl, J. 2017. A check-dam to measure debris flow-structure interactions in the Gadria torrent. In: M., Mikoš, Ž., Arbanas, Y., Yin, K., Sassa (eds.), Advancing Culture of Living with Landslides-Volume 5: Landslides in Different Environments. Springer International Publishing, pp. 465-471.

Schenato, L., Pasuto, A., 2021. On the Use of Optical Fiber Sensors for Debris Flow Monitoring: A Review of Recent Achievements. Belt and Road Webinar Series on Geotechnics, Energy and Environment pp. 60-70.

C6: Some other studies have investigated the link between seismic radiated energy and characteristic flow parameters. e.g.

- *Belli, G. et al., 2022. Infrasonic and Seismic Analysis of Debris-Flow Events at Illgraben (Switzerland): Relating Signal Features to Flow Parameters and to the Seismo-Acoustic Source Mechanism. Journal of Geophysical Research: Earth Surface 127, e2021JF006576. doi.org/10.1029/2021JF006576*

R6: Thank you for the professional comment deeply. A study has investigated the link between seismic radiated energy and characteristic flow parameters: Belli et al. (2022) proposed that physical parameters of debris flow like front velocity, maximum depth, peak discharge and peak mass flux show a positive correlation with both infrasonic and seismic maximum root mean square amplitude, seismic signals characterize with a constant peak frequency instead of magnitude of the flow but infrasound peak frequency decreases when flow velocity, depth and discharge increase.

Reference:

Belli, G., Walter, F., McArdell, B., Gheri, D., Marchetti, E., 2022. Infrasonic and seismic analysis of debris‐flow events at Illgraben (Switzerland): Relating signal features to flow parameters and to the seismo-acoustic source mechanism. J. Geophys. Res.-Earth Surf. 127(6), e2021JF006576.

C7: It is not clear to me how your work is different / innovative in comparison to other studies using seismic signals to investigate debris flows dynamics.

R7: We thank the reviewer for this helpful comment. Our work is different / innovative has been modified in last paragraph of introduction, as follows:

Lines 177 to 182

The study offers a framework for establishing debris flow monitoring and semi-quantitative analysis based on seismic signals. It introduces a cost-effective, dependable, and convenient approach for monitoring debris flows in intricate mountainous terrains, where insufficient sunlight impedes the normal functioning of solar-powered monitoring equipment.

C8: l.80-81: The determination of rainfall threshold is precisely based on the analysis of past events, even if rainfall data come from real-time rainfall data measurements, so I don't understand your point. How would you define, in real time, rainfall thresholds? Alarms using these thresholds must use real-time rainfall data or rainfall prediction, but this is different from defining the thresholds.

R8: Thank you for spending the time to review and assess our manuscript. Rainfall threshold comes from analysis of rain dataset of past debris flow events and can't lie

on real-time rainfall, which is used to evaluate value of rainfall triggering the current debris flow. Rainfall of past events can be used to study the threshold, but real-time rainfall is used to evaluate whether debris flow event occurred and alarms need to be raised based on the threshold.

C9: l.81-82: "the transferability … is poor". You should give more precisions, do you mean that it is difficult to transfer rainfall threshold established for one site, to another site? If yes, give references.

R9: Thank you so much for the comments and we cannot agree more. It is difficult to transfer rainfall threshold established for one site, to another site. Cui et al. (2018) summarized different values of rainfall thresholds for 5 different region and his study region in Fig. 17 of the paper. It can support "the transferability … is poor".

C10: l.83-100: Be more precise in this paragraph on the other kinds of debris flow instrumentation methods.

R10: We deeply appreciate the reviewer carefully went through the manuscript line by line. The paragraph has been modified, as follows:

Lines 92 to 97

Flow depth and velocity can be effectively measured using radar and ultrasonic instruments (Arattano and Moia, 1999; Kogelnig et al., 2014). A key advantage of this approach is that the early warning threshold (e.g., debris flow occurrence) can be easily determined (Arattano and Marchi, 2008). However, a notable drawback is the installation difficulty, particularly in positioning ultrasonic sensors above the channel.

Lines 105 to 110

Currently, a diverse array of instruments, including infrasound sensors (Marchetti et al., 2019), LiDAR (Aaron et al., 2023), fiber optic sensors (Schenato and Pasuto, 2021; Huang et al., 2012), pressure sensors (Berti et al., 2000; Kean et al., 2012), and normal or shear stress sensors (McArdell et al., 2007; McCoy et al., 2010; Nagl and Hübl, 2017), is being increasingly utilized. These devices are adept at capturing an extensive range of parameters, such as infrasound signal amplitudes, velocities of surfaces and fronts, pressure, stress, among others.

C11: l.92-95: It is expected that debris flows have different characteristics and not always the same depth, velocity and peak flow discharge. I think the study of Hürlimann et al. did not show that only.

R11: Thanks a lot for the constructive comment. A sentence has been added after the sentence, as follows:

Lines 100 to 103

In a study of a channel at Illgraben in the Swiss Alps, Hürlimann et al. (2003) showed three debris flows had different properties, such as flow depth, flow velocity, and peak flow, and highlighted the effectiveness of ultrasonic and radar devices in monitoring these debris flows.

C12: l.145: "humid climate", be more specific, what are typical monthly precipitations depending on the time of the year?

R12: Thank you for your helpful comments. "Humid climate" means climate with annual abundant rainfall. It has been modified, as follows:

Lines 190 to 191

Most of the area has a humid climate with annual abundant rainfall of 800-1200 mm (Guo et al., 2016).

C13: l.149-151: Give references for the occurrence of many debris flows in recent years.

R13: We totally agree with the reviewer's suggestion. It has been modified, as follows:

Lines 195 to 201

In recent years, the watersheds have been the sites of numerous debris flow events, posing significant threats to nearby villages, road infrastructure, and hydropower stations. Notable incidents include 17 occurrences documented by Guo et al. (2016) in Table 2, along with specific events such as the debris flow in Ergou on July 10, 2013 (Guo et al., 2016), in Fotangbagou on the same date (Cao et al., 2019), and another in Ergou on July 5, 2016 (Cui et al., 2018), among others.

Reference

Cao, C., Yu, B., Ma, E.L., Liu, S., 2019. Study on debris flow in Fongtuba Gully after the earthquake at Wenchuan County of Sichuan Province. Journal of Sediment Research 44(1), 38-43 (in Chinese).

C14: l.161-162: " a circulation area … to 12°", what do you mean? What is a circulation area? How does it relate to an angle?

R14: Thank you for your professional comments deeply. "Circulation area" means transportation area. Guo et al. (2016) explains Ergou ranges from 5° to 12° in the

debris flow transportation region. Thus, it means longitudinal gradient of the channel is from 5° to 12°. It has been modified, as follows:

Lines 208 to 210

It ranges in altitude from 930 to 4120 m, has a channel length of about 12 km, the average slope of about 12°, and a debris flow transportation area of between 5 to 12° (Guo et al., 2016).

C15: l.175-191: You should be more precise in the description of the instrumentation.

- What is the frequency range (or corner frequencies) of optimal response for the Chengdu Baixinyuan seismometer?
- I guess the eigen frequencies for the geophone are corner frequencies?
- You speak of infrared cameras but during daytime you don't use infrared images, do you? You must be clearer on this point. Besides, you must specify that you record still images and not videos at 5-min intervals.
- The technical characteristics of the camera must be more precise, including in particular the angular field of view and the lens.
- Are all data recovered in real time through internet / GSM?

R15: Thanks a lot for the constructive comment. The description of the instrumentation has been added, as follows:

Lines 228 to 249

We have devised a near-field debris flow monitoring system, which includes seismic monitoring equipment, an infrared camera for observing the flow regime of debris flow, and a rainfall gauge. This system is a cost-effective, dependable, and convenient solution for monitoring debris flows. It primarily relies on seismic signals, an approach particularly advantageous in complex mountainous areas where the scarcity of sunlight limits the availability of solar energy for powering monitoring equipment. Infrared cameras with 5-min interval shooting have a lower electric power consumption than infrared videos with better infrared monitoring range and higher resolution, which is available in our study area. Hikvision's infrared video camera (Type: DS-2CD3T46WDV3-L) exhibits high power consumption. The power generated by the solar panel is only sufficient to sustain continuous video monitoring for approximately 74 hours. In instances of prolonged cloudy and rainy weather lasting more than three consecutive days, the camera faces challenges due to insufficient solar energy supply, hindering its ability to maintain uninterrupted video monitoring. In contrast, other infrared cameras with a 5-minute interval shooting mode have been consistently monitoring the debris flow channel from June to October

in both the years 2021 and 2022. These cameras are equipped with a combination of solar cells and eight 1.5-volt dry cell batteries, enabling them to sustain monitoring operations for an impressive duration of 18 months.

Two monitoring stations for each gully can get a seismic signal, rainfall, and infrared imagery to analyze semi-quantitatively characteristic of the debris flow process at two different locations of the gully.

1. Chengdu Baixinyuan Science Technology Company Limited has not provided information about the frequency range (or corner frequencies) of optimal response for the seismometer.

2. The eigen frequencies are ground velocity response of signal output for the geophone. The eigenfrequency which is used to explain range of accurate recording can be considered as corner frequencies because they have a strongly similar definition. It has been modified, as follows:

Lines 256 to 260

In Ergou Gully, seismic monitoring (Geophone) and acquisition (Data-Cube) equipment, provided by the Helmholtz Potsdam Center and German Geoscience Center, was used with a sampling frequency of 100 Hz and an eigenfrequency of 4.5–150 Hz, i.e., ground velocity response of signal output.

3. Infrared cameras have been used not to shoot infrared images but ordinary images during daytime. Infrared cameras record images instead of videos at 5-min intervals. It has been modified, as follows:

Lines 261 to 264

Each observation station was also equipped with an infrared camera to record the images of the debris flow at 5-minute intervals in real time to provide particle size data and insights on the debris flow processes to compare with the seismic observations.

4. The angular field of view and the lens is 120° for infrared cameras. It has been modified, as follows:

Lines 264 to 267

The cameras have several tens of meters of visibility at 2592×1944 dpi resolution in the daytime and about 2 to 4 m visibility at 1920×1080 dpi resolution at night, and the angular field of view and the lens is 120° for infrared cameras.

5. All data are recovered in real time not through internet/GSM, because the observation stations have no network signal to link internet to transmit data. It has been modified, as follows:

Lines 267 to 269

All data are collected in real time but not through internet/GSM, because the observation stations have no network signal to link internet to transmit data.

Methodology

C16: The workflow is not clear in Figure 3. If I understand well, the "absorption attenuation compensation" (consider changing the name to simply "attenuation compensation") depends on the frequency, so you need to apply the STFT first. Besides, the PSD is deduced from the time frequency power spectrum, so the correct workflow should be, if I understand well, as in the following graph. The order of subsection in the Methodology section should reflect this ordering. Finally, if I'm correct you do not explain what the "amplitude method" is and what the "simplified signal" is.

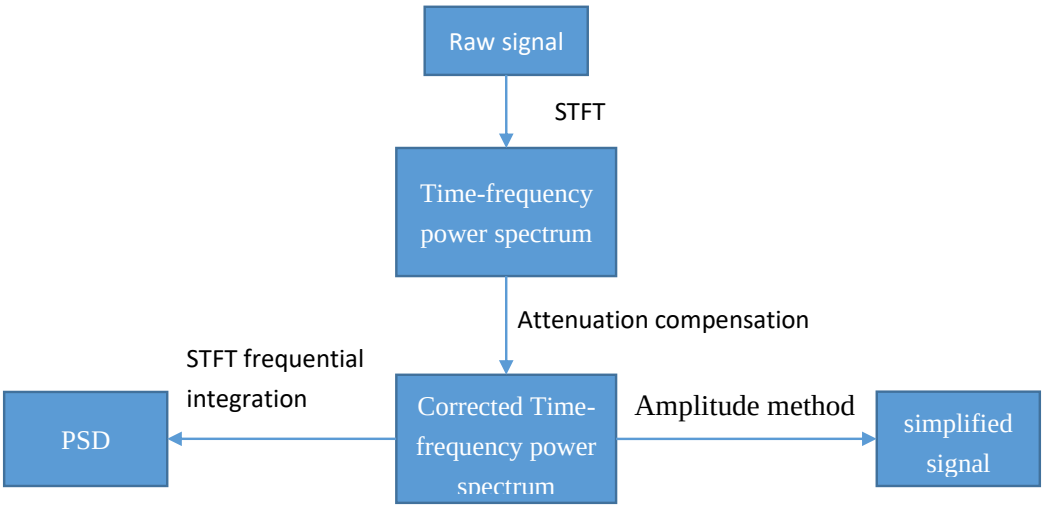

R16: Thank you for the constructive advice. Actually, power spectral density curve, time-frequency power spectrum, simplified signal are obtained based on original signal, which differs from your workflow. We acknowledge the workflow is not clear to make you confused, so the workflow of Fig. 3 has been modified into the following graph after we changed the structure of the manuscript. And we start the section Methodology with a brief systematic introduction to this section to facilitate the reader's understanding of our Methodology. This part has been modified, as follows:

Lines 279 to 295

To extract information on debris flow evolution, debris flow seismic signals were processed and interpreted by following the procedure in Fig. 3. Absorption attenuation compensation is first to be processed for each frequency of the extracted seismic signal of debris flow to restore the different energy loss caused by different propagation, which was aimed to obtain the seismic signal of debris flow that is not affected by sensors installation location. Then, the seismic spectrogram is from compensated seismic signal based on short-time Fourier transform, characteristic analysis of debris flow evolution has been done by computing power spectral density of keyframe and the absolute value of time-domain amplitude, the evolution analysis result has been verified based on infrared imagery and post-event field investigation. Finally, the maximum velocity of debris flow has been estimated by computing the absolute seismic amplitude of different monitoring stations based on the cross-correlation function, which has been verified by the Manning formula. The key steps are outlined below in Fig. 3. Amplitude method in this figure is used to get the absolute value of time-domain amplitude in this figure. After this method, the signal processed by us is called a simplified signal.

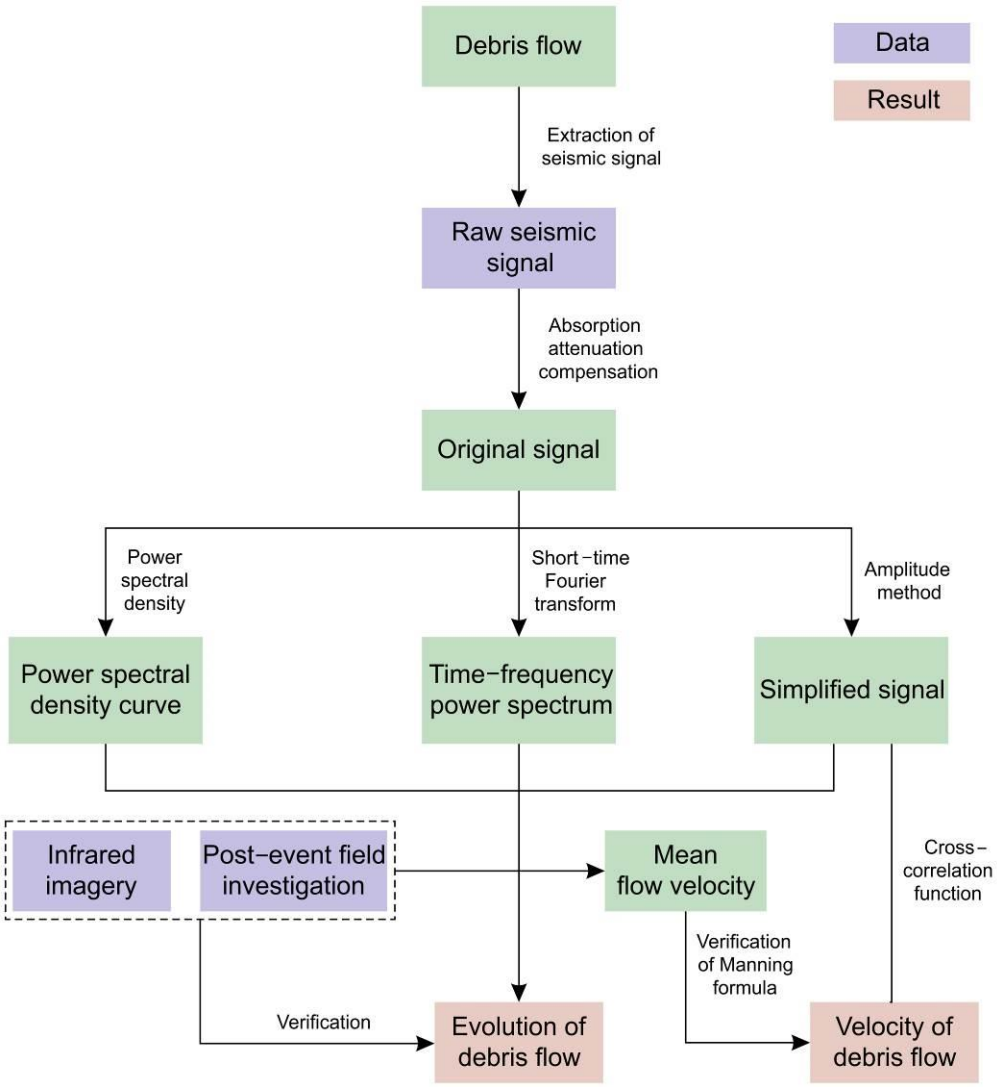

Fig. 3. Research methodology for processing and analysis of debris flow seismic signal.

C17: You should explain, at least briefly, how equation 8 was derived by Lai et al. (2018). I'm surprised that the solid fraction is not taken into account, why is that? The work of Farin et al. 2019 include a dependence to solid fraction, although they reckon it is of second order compared to the influence of velocity and characteristic particle diameter (see their equation 24). In any case, their study could be mentioned, especially as they specifically discuss the possibility to estimate flow velocity from seismic data. See also their figure 7 where they compare their model to the one of Lai et al. (2018) used in your study.

- *Farin, M. et al., 2019. A physical model of the high-frequency seismic signal generated by debris flows. Earth Surface Processes and Landforms 44, 2529–2543. doi.org/10.1002/esp.4677*

R17: We thank the reviewer for this helpful comment. Eq. (7) only can provide an order of magnitude estimation of PSD of debris flow event, which offer important insight about debris flow characteristic. Indeed, solid partial fraction affected seismic strongly. Solid partial fraction is the same as the velocity of debris flow, whose contribution to PSD is three cubed, and there are many documents about its discussion. The purpose of our research is to establish a relationship between PSD of seismic signal and dynamic parameters of debris flow. We used simple Eq. (7) to achieve semi-quantitative analysis. However, when we used result of Farin et al. (2019) to estimate velocity, the estimation has less reliability because of near-field monitoring and difficulty of parameters measurement during propagation. Thus, we did not mention this result in our study. The mathematical model we observed in the field is further studied in our subsequent research, near-field monitoring used a non-linear solution integration model, which has a difficult computation. After that, we can achieve quantitative estimation of velocity and grain size.

Reference

Farin, M. et al., 2019. A physical model of the high-frequency seismic signal generated by debris flows. Earth Surface Processes and Landforms 44, 2529–2543. doi.org/10.1002/esp.4677

C18: You could also mention and discuss existing work linking seismic PSD to bed load transport in rivers, but maybe that does not apply to debris flows? E.g.:

- *Roth, D.L. et al., 2016. Bed load sediment transport inferred from seismic signals near a river. Journal of Geophysical Research: Earth Surface 121, 725–747. doi.org/10.1002/2015JF003782*

R18: Thank you for spending the time to review and assess our manuscript. PSD is associated with the transport of bedload in rivers. Roth et al. (2016) provide an insight that the component signals originate from water turbulence, precipitation and sediment transport. It gives us a research direction about studying PSD of debris flows. The two above sentences have been added, as follows:

Lines 356 to 359

PSD has a link with transporting bed load in rivers, Roth et al. (2016) provide insight into that the component signals come from water turbulence, rainfall, and sediment transport. It gives us a research direction about applying PSD to studying debris flows.

References:

Roth, D. L., Brodsky, E. E., Finnegan, N. J., Rickenmann, D., Turowski, J. M., Badoux, A., 2016. Bed load sediment transport inferred from seismic signals near a river. J. Geophys. Res.-Earth Surf. 121(4), 725-747.

C19: On another point, despite what you write in Figure 4, the seismic signals you use are not raw. To get velocities, you need to deconvolve the raw electric signal. How did you do it? To do it you certainly had to filter the signal, what frequency band did you use?

R19: Thank you so much for the comments. Velocity is not debris flow velocity but vibration velocity of seismic amplitude. In fact, we haven't deconvolved the raw electric signal. At the same time, we also have not filtered the signal, but the signals have been filtered from Fig. 6, 7, 9, 10, 11. Only Fig. 5 showed raw signal instead of filtered signal.

C20: It is not clear to me how you quantify the flow velocity, the flow rate, and the particle content from the pictures taken by the camera. You should explain more clearly.

R20: We thank the reviewer for this comment. In fact, after changing structure of the manuscript and research purpose, we can only achieve semi-quantitative analysis of flow velocity, the flow rate, and the particle content from the pictures taken by the camera. We cannot quantifying of these parameters only use images from camera since the PIV technics cannot be used for images with 5 minutes interval.

C21: l.209-210: Did you implement yourself the STFT or did you use existing implementations, using the Fast Fourier Transform? If you implement it yourself and re-coded the FFT, you should say so and say what FFT algorithm you used. Otherwise, say what programming function / language you used.

R21: Thanks a lot for the constructive comment. We did not recode the Fast Fourier Transform but build-in function spectrogram of MATLAB to achieve STFT directly. This sentence has been added at the end of Section 3.1, as follows:

Lines 305 to 306

A built-in function "spectrogram" of MATLAB is used to achieve STFT directly from the software manual.

C22: l.214-222: Your explanation is misleading. The time delay you compute is not related to the propagation of the signal from a single source, with a given wave velocity. Instead, you consider that the signal recorded at a station corresponds to the passage of a mobile source in front of the station. Thus the time delay computed by cross correlation corresponds to the travel duration of the source between the station, and not the wave travel duration. This should be more explicit.

R22: Thank you for your helpful comments. Our explanation is misleading indeed. The description about cross-correlation function has been modified in Section 3.2:

Lines 308 to 312

The cross-correlation function is used to compute the time delay of τ that corresponds to the travel duration of the source between the stations. The time delay of the signals comes from sampling signals, such as M signal samples $[x_K]$, $[y_K]$ in Eq. (2) and (3) at different locations when the maximum calculation result $\phi_{yx}(\tau)$ is obtained based on Eq. (4) (Arattano and Marchi, 2005).

Reference:

Comiti, F., Marchi, L., Macconi, P., Arattano, M., Bertoldi, G., Borga, M., Brardinoni, F., Cavalli, M., D'Agostino, V., Pennna, D., Theule, J., 2014. A new monitoring station for debris flows in the European Alps: first observations in the Gadria basin. Nat. Hazards 73, 1175-1198.

C23: l.227-229: Why don't you also compare it to the velocity derived from the combination of equations 7 and 8?

R23: Thank you for the constructive comments. If the velocity can be determined based on Eq. (6) and (7), the diameter as a variable should be also determined. We

only know the diameter of 94% for the grain sample, but the grain diameter of debris flow cannot be acquired. Thus, we cannot get the velocity from Eq. (6) and (7).

C24: l.231-232: You must explain more clearly what J and R are, explain how you compute them, and illustrate it on a figure (e.g. on current Figure 13 that could be placed in section 3.3).

R24: We deeply appreciate the reviewer carefully went through the manuscript line by line. Section 3.3 has been modified, as follows:

Lines 322 to 346

To verify the reliability of the velocity calculations based on the cross-correlation function, mean velocity was also determined using the Manning formula (Eq. (5)), which was originally developed for hydraulics problems (Rickenmann, 1999). The formula is used to calculate the mean flow velocity of a debris flow passing through a section based on characteristic terrain parameters of the section (Yu and Lim, 2003; Cui et al., 2013; Guo et al., 2016):

$$v = \frac{1}{n} J^{\frac{1}{2}} R^{\frac{2}{3}}, \quad (5)$$

where v represents debris flow velocity, n represents the roughness coefficient of the channel, J is the slope of the section in percentage instead of a degree, and R represents the hydraulic radius, calculated by dividing the area of the monitoring section (as determined by the DSM) by the wet perimeter, denoted as χ (Fig. 4). Channel parameters were extracted from cross-sections at the monitoring stations (Fig. 4). A key element of the Manning formula is the channel roughness coefficient n (Smart, 1999), which was determined as 0.05 (Xu and Feng, 1979) for the Fotangbagou gully. The gradient ratio J of the monitoring section was determined using the digital surface model (DSM) output of the UAV aerial survey. The values for two cross-sections are 0.13. χ can be employed as a means to estimate the cumulative bed length and lateral depth of the channel that is inundated by debris flow within the cross-section. For the cross-section of monitoring station 1, the area of the monitoring section and the wet perimeter χ are 17.7 m^2 and 14.2 m, respectively. For another cross-section, the two values are 27.5 m^2 and 21.6 m, respectively. Thus, two values of the hydraulic radius R are 1.25 m and 1.27 m for the two monitoring stations.

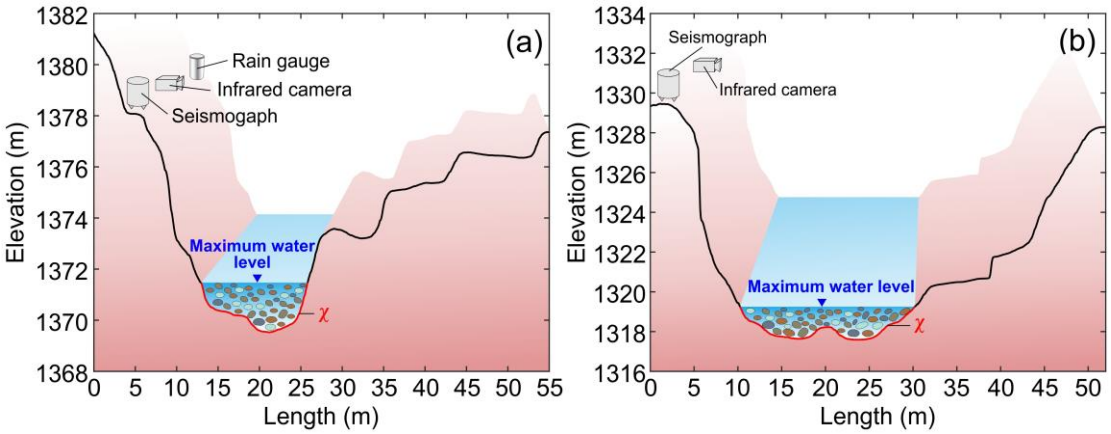

Fig. 4. Cross-sections of Fotangbagou gully showing maximum water level used in calculation of mean velocity by the Manning formula. (a) Monitoring station 1; (b) Monitoring station 2.

Reference

Smart, G.M., 1999. Coefficient of friction for flow resistance in alluvial channels. Proc. Inst. Civil Eng.-Water Marit. Energy 136(4), 205-210.

Xu, M.D., Feng, Q.H., 1979. Roughness of debris flows. Proceeding of the First Conference of Chinese Research of Debris Flows, pp. 51-52 (in Chinese).

Yu, G., Lim, S.Y., 2003. Modified Manning formula for flow in alluvial channels with sand-beds. J. Hydraul. Res. 41(6), 597-608.

C25: l.233: Explain how d50 is chosen.

R25: Thanks a lot for the constructive comment. Actually, *n* for Fotangbagou gully is determined as 0.05 empirically (Xu and Feng, 1979). It has been modified, as follows:

Lines 332 to 334

A key element of the Manning formula is the channel roughness coefficient *n* (Smart, 1999), which was determined as 0.05 (Xu and Feng, 1979) for the Fotangbagou gully.

C26: l.236-247: It is not clear in this paragraph how the two expressions of the PSD in eq 7 and 8 will be used and combined to extract information of the debris flow. As I see it, eq 7 allows to compute the PSD, and then eq 8 can be used to invert for the velocity, which is extremely useful in practice for monitoring if you have only one station and cannot measure travel duration between two stations! You must clarify this point.

R26: Thank you for the useful advice. Eq. (6) is used to calculate the PSD and Eq. (7) is used to analyze the velocity and grain size with PSD of the debris flow between the two stations, as there are no continuous time series between the two stations. The sentence has been added in the end of Section 3.4, as follows:

Lines 374 to 377

Eq. (6) is used to compute the PSD and Eq. (7) is used to analyze velocity and grain size with PSD of the debris flow between the two stations due to lack of data of continuous time series between the two stations.

C27: l..239: How do you choose in practice fmin and fmax?

R27: We thank the reviewer for this helpful comment. A sentence is added to explain it, as follows:

Lines 354 to 355

The sampling rate is 100 Hz, so we choose 1 Hz and 50 Hz (i.e., a half of 100 Hz) as f_{min} and f_{max}.

C28: l.243-247: You should explain how the different fixed parameters (L, W, D, vc, r0, xi, Q) are chosen, and specify that f and u are the variable parameters (if I'm correct).

R28: Thank you for spending the time to review and assess our manuscript. It should be explained how the different fixed parameters L, W, f, v_c, r_0, ξ, Q are chosen, and specify that D and u are the variable parameters. It has been modified in Section 3.4, as follows:

Lines 365 377

Width W of the river channel is about 10 m. We will take the monitoring station as the center, the upstream and downstream 10 m range of the river as the main source of the monitoring station; Then, the river channel is divided into 200 segments at an interval of 0.1 m, and the travel time from each segment to the station is calculated respectively. Then, the geometric average value of the 200 segment travel times is calculated, which is taken as the average value of the travel time. Using the second Fotangbagou debris flow as an example, Q is 4 and 2.4 for monitoring points 1 and 2, the horizontal distance between the channel and monitoring station is 15 m and 25 m, and the Rayleigh wave velocities of 800 m/s and 500 m/s at 1 Hz, respectively (Guo et al., 2023). So, the seismic travel time of 0.02s and 0.04s respectively. Eq. (6) is used to compute the PSD and Eq. (7) is used to analyze velocity and grain size with PSD of the debris flow between the two stations due to lack of data of continuous time series between the two stations.

Reference

Guo, N., Zhou, X., Xu, K., Wang, Y., Lyu, J, Duan, M., 2023. Near-surface *Q*-value survey method based on uphole with hammer excitation and receiving using multi-stage geophones on wells. Oil Geophysical Prospecting 58(2), 295-304 (in Chinese).

C29: l.252 eq 9: You should explain more clearly how this damping factor is used. What data do you correct and how? The Time-Frequency power spectrum?

R29: Thank you for your useful advice. We have explained more clearly how this damping factor is used in Eq. (8). It has been modified, as follows:

Lines 387 to 392

Eq. (8) is used to characterize the attenuation of plane waves absorbed by the earth. In this equation, t represents the propagation time of the seismic wave, a key parameter Q represents the attenuation factor quantitatively depicting the absorption attenuation, $h(t,f)$ represents the relative amplitude attenuation at the frequency-domain spectrum of the original seismic wave at a certain frequency f after the propagation time t.

C30: l.258 eq 10: It is not clear how equations 10 and 9 are combined. Do you always use eq10, or do you use it only when "the amplitude at a certain frequency has decayed greater"? I don't understand what it means, you should be clearer.

R30: Thank you for your useful advice. Computation result of Eq. (9) must depend on result of Eq. (8). It has been modified, as follows:

Lines 397 to 399

The high-frequency signal can be restored by Eq. (9) better with a comparison of Eq. (8). Because the seismic signal of debris flow belongs to a high-frequency signal, we always use Eq. (9) at all the frequencies of 1 Hz to 50 Hz actually.

C31: l.259: How is sigma chosen?

R31: Thanks a lot for the constructive comment. The main criteria for the value of the parameter is that the signal-to-noise ratio of seismic after compensation is relatively controllable, that is, the signal-to-noise ratio of seismic after compensation will not greatly reduce. We have modified the sentence, as follows:

Lines 395 to 396

where σ is a constant named stability control factor, whose value comes from numerical experiment., with a σ^2 value of 0.02 used here.

C32: Are you sure your signal is correct up to 50Hz, provided that your sampling frequency is 100Hz, such that 50 Hz is really the upper bound of what you can theoretically investigate. I'm not an expert in seismology, but I'd be confident for frequencies below 40 or even 35 Hz only. Besides, in figures of time-frequency spectra, there seems to be a cutoff at 42-45 Hz: does it correspond to a signal filtering?

R32: Thank you for your constructive comments. We are sure signal is correct up to 50 Hz and 50 Hz is the upper bound of signal indeed. We didn't use signal filtering in Fig. 5. After this figure, signals have been used signal filtering in other figures that contain seismic signal.

C33: l.266-270 You should explain more clearly how you determine de beginning time of the events (it is not self-evident, as we can see an emerging onset in Fig. 4), and the frequency bands. What are the criteria to determine the limits?

R33: We totally agree with the reviewer's suggestion. Beginning time of the events are determined by sudden increase of time domain signal and spectrogram. Meanwhile, we also asked locals about the time for a rough verification. Nevertheless, infrared imagery can be considered to confirm starting time for the second debris flow of Fotangbagou. The sentences above have been added in the first paragraph of Section 4.1, as follows:

Lines 403 to 407

We have identified three debris flows by consulting with local residents to confirm the occurrence of these events. Through the methods described above, we can confidently distinguish these three events as debris flows rather than intense sediment transport events. It is important to note that our determination did not rely on critical rainfall thresholds as a method of assessment.

Lines 414 to 417

The beginning time of the events is determined by a sudden increase of the time domain signal and spectrogram, asking locals about the time. Besides, infrared imagery can be considered to confirm the starting time for the second debris flow of Fotangbagou.

C34: l.285: "a large intensity of precipitation", in comparison of what is it large? What are typical duration/intensities of precipitations in the area, at his time of the year?

R34: We deeply appreciate the reviewer carefully went through the manuscript. The annual average precipitation is 1200 mm in study area (Cui et.al, 2018). June to August is typical duration of precipitations in the area. Due to lack of related

intensities of precipitations, it can be said to "a large intensity of precipitation", so it has been modified into "precipitation". It has been modified, as follows:

Lines 432 to 434

The analysis of rainfall data indicates the presence of precipitation preceding the onset of the three debris flows. Furthermore, the rainfall data can be examined in terms of its initiation time and the time of significant amplitude changes in seismic signals.

C35: l.286: "the rainfall data coupling … by seismic signals". I don't understand this sentence.

R35: Thanks a lot for the constructive comment. This sentence means that rainfall data can be analysed in the starting time, time of signal amplitude change (increase or decrease) from seismic signals. The sentence has been added to explain it clearly, which is shown in R34 for reviewer 1 from lines 432 to 434.

C36: l.288: "hourly rainfall maxima", what is the period considered to determine the maxima? If this is just the period displayed in Figure 5, you may well have bigger precipitations before…

R36: Thank you for the useful advice. "Hourly rainfall maxima" refers to "hourly rainfall maxima on the day of debris flow eruption". It has been modified, as follows:

Lines 435 to 438

Initiation of the two debris flows in Fotangbagou Gully coincided with hourly rainfall maxima on the day of debris flow eruption (second highest and highest) of the 24 h period, but the Ergou Gully debris flow did not correspond with an hourly rainfall maximum.

C37: l.301-313: Be more explicit by saying it is complex in practice to take into account the linear distribution of seismic sources. Thus, you only consider the source at the immediate proximity of the sensor (if I understand well). Besides this whole part should be in the Methodology section, not in the Results.

R37: We thank the reviewer for this helpful comment. Actually, the source at the immediate proximity of the seismic monitoring equipment was considered by us. C37 is similar to C28, a part of Line 301-313 has been removed into the Methodology section. Thus, we remove the rest part of Line 301-313 into the Methodology section, Section 3.4.

C38: l.306-307: "River channels are … processing signal". What do you mean?

R38: Thank you for spending the time to review and assess our manuscript. The sentence means that the width of the river channel is 10 m between monitoring station 1 and 2. It has been modified into the sentence in Section 3.4, as follows:

Line 365

Width *W* of the river channel is about 10 m.

C39: l.316-317: "The characteristic change … is more obvious". This is not clear, what do you mean? I don't understand the "similarity" you mention, and what is "more obvious".

R39: Thank you so much for the comments. The sentence means that increase and decrease of two time-domain curves are more similar after compensation, and their characteristics change is more obvious. "Similarity" means amplitudes of the two curves increase or decrease similarly. "More obvious" means it is a little bit difficult to discover similarity of the two curves before compensation, but similarity of the curves become more obvious after compensation. It has been modified, as follows:

Lines 450 to 452

Moreover, when analyzing the time domain curve, we observe noticeable enhancements in the characteristics of the curve after site two's compensation, further enhancing the similarity to site one.

C40: l.318: "From the perspective of effect", what do you mean?

R40: We thank the reviewer for this comment. "From the perspective of effect" means "from result of the compensation". It has been modified, as follows:

Lines 452 to 454

In terms of effectiveness, the compensation demonstrates favorable outcomes, effectively reducing the impact of absorption and attenuation on the debris flow seismic signal.

C41: l.319: "the compensation effect is relatively good", what do you mean? How do you define that is "relatively good"?

R41: Thanks a lot for the constructive comment. "Relatively good" cannot be quantified because there is single monitoring station. It is an empirical evaluation method, the general evaluation criteria are high-frequency energy is compensated. the noise of the compensated seismic signal has little effect on the effective signal, the principle used in the compensation process is to compensate for the loss of high-frequency energy as much as possible under the condition that the overall signal-to-

noise ratio of the signal is relatively controllable. In order to reduce the ambiguity of the reader's understanding of this issue, we rewrite the original text which is shown in R40 for reviewer 1 from lines 452 to 454.

C42: Figure 6: Why is there a maximum for the damping factor in Fig 6e and not 6a?

R42: Thank you for your professional comment. Parameters in $h(t,f)$ are different for the two stations, which caused the curve change of $h(t,f)$ are different for the two station. Thus, there is a maxima for the damping factor in Fig 6e and not 6a.

C43: l.347-348: You speak of frequency bandwidth but do not give frequency ranges. To what do the values 8 Hz, 43 Hz and 22 Hz correspond?

R43: We totally agree with the reviewer's suggestion. "Frequency bandwidth" is used mistakenly. Actually, the word has been modified into "frequency of high power corresponding to red or dull-red". 8 Hz and 43 Hz refer to lower and upper frequency limit of relative high power that is red or dull-red in color bar during the initiation of debris flow. 22 Hz refers to a main frequency of high power that is red or dull-red in color bar in the end of debris flow. The sentence has been modified, as follows:

Lines 479 to 482

While the frequency associated with high power, represented by the colors red or dull-red, exhibited a rapid increase from 8 to 43 Hz following the initiation of the debris flow and maintained a high power at 22 Hz, indicated by the colors red or dull-red, until 8:45.

C44: l.350: You mention an amplitude peak at 7:45 but there is another one at 8:20.

R44: Thank you for your professional comment sincerely. An amplitude peak at 8:20 is possibly impact between stones in the debris flow around monitoring station 2.

C45: l.359-362: You must quantify more precisely your statements.

R45: Thanks a lot for the constructive comment. After changing structure of the manuscript, we can only achieve semi-quantitative analysis. The frequency and amplitude differences of these two stations have been explained in the previous part. This step is to summarize the above objective data, mainly to express that the frequency and amplitude of seismic signal are different because geological conditions near the two stations of the same gully are also different, but changes in frequency and amplitude characteristics tend to be consistent.

C46: l.362: what is the "absolute average amplitude"? A graph of the temporal variations of the PSD would help visualize the sharp increase and slow decrease you mention, as well as characterizing the durations of these phases.

R46: Thank you for the useful advice. "Absolute average amplitude" refers to simplified signal in Fig. 3. It is the word we forgot to delete, so the word has been deleted. After consideration, spectrogram will achieve the result mentioned by you, so it is not a necessity to draw a graph of the temporal variations of the PSD.

C47: l.365 and following : As written previously, it not clear at all to me how you can quantify flow velocity, flow rates and solid content from still pictures. You give only qualitative indications, and thus results remain quite vague. Besides, the pictures in Figure 8 are very small, and I can't really see a difference between them, even qualitatively.

R47: We thank the reviewer for this helpful comment. This data is sampled for 5-min interval. We cannot clearly see changes in flow velocity like video, but we empirically analyze the velocity, discharge, and particle content of a sampling site through semi-quantitative estimation: Velocity can be estimated by flow state like turbulence or not in relative smooth part (point C in Fig. 7). The discharge of debris flow can be estimated by the area of the channel occupied by the debris flow. For example, there is flow at point A and concave bank at 7:39, and point A will be submerged at 7:44. The form of water flow is identified. Particle content can be estimated by the color of debris flow. The darker the color is, the higher the particle content will become.

C48: l.409-411: Is this passage about the role of the erosion an interpretation of what you see, or do you have data to support this?

R48: Thank you for spending the time to review and assess our manuscript. We used infrared camera with lower power consumption to monitor debris flow to achieve semi-quantitative analysis. In the subsequent research, we will consider high resolution camera. We have modified context about erosion, as follows:

Lines 544 to 559

Analyzing the evolution of the debris flow, we observed a gradual increase in debris flow discharge from 7:39 to 7:59. This increase can be attributed to the relatively high flow velocity during this period, leading to intensified erosion along the course of the rock and soil body adjacent to the accumulation area. As a result, the fluid-solid phase material content increased, leading to a tendency for the flow rate to rise. At 7:59, the flow velocity decreased to some extent, resulting in weaker erosion. The debris flow

gradually transitioned into a state resembling a “flood”. In Fig. 7f, point A exhibits a stationary stone block that cannot be moved, and in Fig. 7g, the rock bed becomes clearly visible. These observations indicate that the erosion capability and carrying capacity of the debris flow were weak at this moment. This complex behavior in the trend of flow velocity, discharge, and particle composition changes during the debris flow’s evolution underscores the inconsistency in their characteristics. In the next section, we will integrate these variables with the seismic PSD forward modeling of debris flow generation to analyze their respective impacts on the signal. This analysis will provide insights into the contradictory peak time observations between infrared imagery and seismic interpretation.

C49: l.412: We cannot see the rock you mention in Figures 8e and 8f, and we cannot say if it was present before or not.

R49: Thank you so much for the comments. In order to support this result, we offer a pre-event, post-event imagery of the channel monitored by an infrared camera, respectively, which is shown in Fig. 7a, 7h.

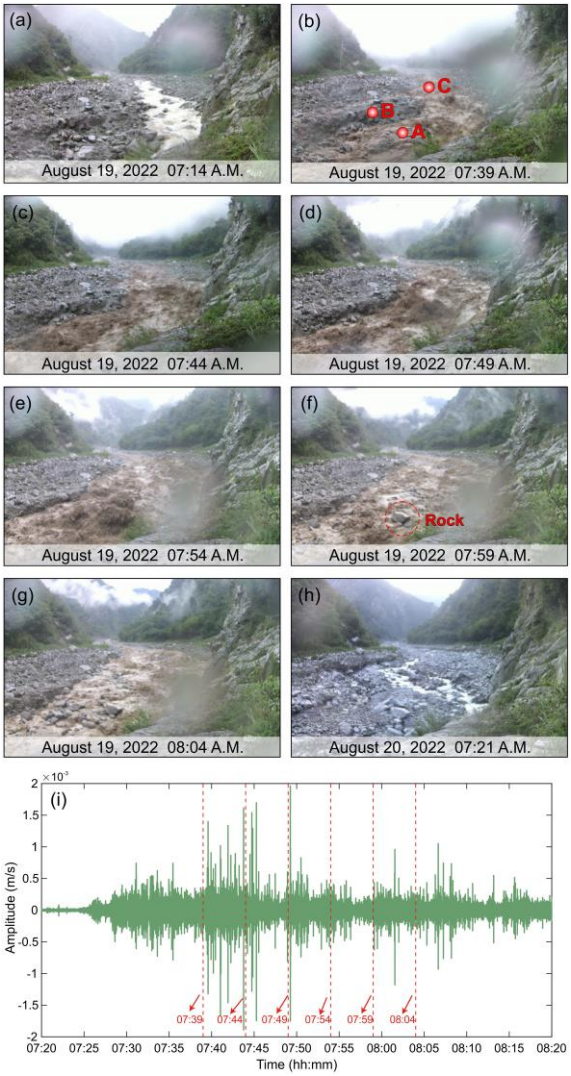

Fig. 7. Infrared camera images and seismic signals were recorded at monitoring point 1 in Fotangbagou Gully during the second debris flow on the morning of August 19, 2022. Images (b)-(g) were recorded every 5 minutes from 7:39 to 8:04: (a) before debris flow; (b) 7:39 frame; (c) 7:44 frame; (d) 7:49 frame; (e) 7:54 frame; (f) 7:59 frame; (g) 8:04 frame; (h) after debris flow. (i) The seismic signal was recorded at the point.

C50: l.418: As the debris fan is in a river, haven't the deposits of the debris flow been eroded by the river?

R50: We thank the reviewer for this comment. We started post-event field investigation on the third day after the debris flow events. Thus, maybe the deposits would be eroded by the river inescapably. We have added speculation of it, as follows:

Lines 597 to 600

The low cohesive sediment content of the accumulation fan sample could be due to removal by post-event processes, either by the flushing action of the Minjiang River or by human clearance of the impoundment fan.

C51: l.422-424: "the rocks at the bottom … are relatively small", did you quantify the spatial variation of granulometry, e.g. by exploiting the DSM from the UAV survey? This would be much better than just a qualitative statement. And you provide only two pictures to support your affirmation, including one without scale.

R51: Thanks a lot for the constructive comment. We cannot quantify the spatial variation of granulometry based on DSM from UAV because the resolution of photography images cannot satisfy it. We can only get the spatial variation of granulometry based on post-event field investigation (comparison with reference objects) and particle size distribution analysis. For subplot (c), we acknowledge it doesn't have scale because we forget to measure rock. We will improve it to do measurement in the subsequent post-event field investigation.

C52: l.429: Did you carry out only one granulometry analysis? To what extent is it representative of the deposits granulometry, given the spatial variations you mention before? Several sample analyses are usually needed to estimate the variability. Besides, you must have done some sieving before the granulometry analysis, can you give more information on that? Did you record the fraction of materials that was above the maximum particle size displayed in the granulometric curve?

R52: Thank you for your constructive comments. We carried out only one granulometry analysis. It can only represent deposits granulometry of the sample. It has been modified in the manuscript, as follows:

Lines 591 to 593

Due to lack of several sample analysis in this study, we should consider finishing several sample analyses to estimate the variability in other researches.

We have done some sieving with different sieves that allow grains of different diameter get through the sieves before the granulometry analysis. It also has been modified in the manuscript, as follows:

Lines 593 to 595

We forgot to record the fraction of materials that was above the maximum particle size displayed in the granulometric curve. Thus, we should finish it in other similar researches.

C53: l.436: The particle size you give is the particle size of your sample, not of the debris flow solid fraction.

R53: We totally agree with the reviewer's suggestion. "Particle size of this debris flow" has been modified into "particle size of the sample", as follows:

Lines 600 to 601

The particle size distribution shows that 94% of the particle size of the sample is 0.018 m, i.e., D in Eq. (7).

C54: l.447: What frequency bandwidth was used to compute the PSD?

R54: We deeply appreciate the reviewer carefully went through the manuscript line by line. We used frequency bandwidth of 50 Hz to compute the PSD.

C55: l.447 to 457: Figure 10 does not illustrate very well what you say in this paragraph, especially the temporal variations you mention. A plot with the temporal variations of the PSD would be more appropriate.

R55: Thanks a lot for the constructive comment. We will follow your constructive suggestion if we choose video to monitor debris flow subsequently. Because we used camera with 5-min interval shooting, it is better to draw a plot with the frequency variations of the PSD to achieve semi-quantitative analysis of PSD.

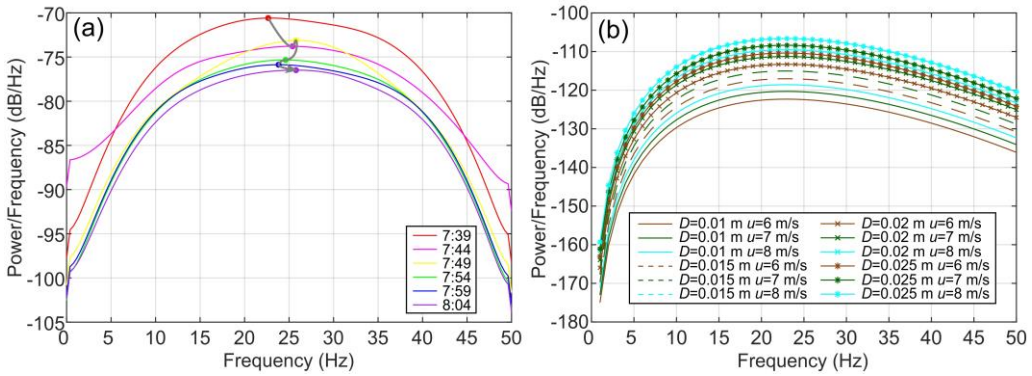

Fig. 9. Characteristic change of power spectral density (PSD). (a) Evolution of PSD during the second debris flow in Fotangbagou Gully on the morning of August 19, 2022, from 7:39 to 8:04; (b) Comparison of PSD for different grain sizes (D) and velocities (u). Each curve represents PSD frequency over 60 s. The six dots in subplot (a) correspond to the PSD maximum at the six-time points from 7:39 to 8:04, and the black arrows indicate the time course of these six-time points. The PSD values of D=0.015 m and u=8 m/s, D=0.02 m and u=6 m/s are equal, so the curves coincide in subplot (b).

C56: l.469-470: I don't understand how you derive the values 0.5, 0.55 and 0.6 from the 94% quantile 18mm.

R56: Thank you for the useful advice. We have modified grain size of 0.5, 0.55 and 0.6 m into grain size of 0.01, 0.015, 0.02 and 0.025 m. It has been added, as follows:

Lines 639 to 640

D was determined based on 94% of the particle size, resulting in values of 0.01 m, 0.015 m, 0.02 m, and 0.025 m, respectively.

C57: l.471: How do you choose the velocity values 2, 4 and 6 m/s ? Why don't you use the granulometry distribution established in Fig 9, the PSD computed from the seismic signal, and eq8, to deduce the velocity?

R57: We thank the reviewer for this helpful comment. We restart to determine the velocity values of 6, 7, 8 m/s to avoid overlap of several curves. It has been modified, as follows:

Lines 640 to 642

The velocity *u* was consistent with the mean velocity described in Section 4.3, which was set at 2 m/s, 4 m/s, and 6 m/s.

The three values are randomly chosen in empirical velocity of debris flow. Because *D* and *u* are variables, we cannot determine the two values based on Eq. (7). Besides, the equation can only achieve semi-quantitative analysis.

C58: l.479-484: I don't understand how you get to the conclusion that u has a greater influence than D on the estimation of the PSD. In equation 8 they are both at the power of 3, so relative variations of u and D result in similar relative variations of the PSD.

R58: Thank you for spending the time to review and assess our manuscript. After we change structure of the manuscript, grain size of 0.01, 0.015, 0.02 and 0.025 m and the velocity values of 6, 7, 8 m/s have been rechosen. Besides, the previous conclusion is obtained based on the previous values of grain size and velocity instead of all the values. It has been modified, as follows:

Lines 646 to 652

As depicted in Fig. 9b, it is evident that the velocity of the debris flow significantly determines the energy level of the PSD, while the particle size exerts a comparatively weaker impact on energy levels than flow velocity. Specifically, for a debris flow with the same particle radius, the energy across the entire frequency band experiences a sharp increase with higher flow velocities. In contrast, the increase in energy within each specific frequency band remains relatively modest when varying particle size at a consistent flow velocity.

C59: l.484: "The influence of … than at the low frequency end", I don't understand how you get to this conclusion.

R59: Thank you so much for the comments. The sentence is used to explain that with comparison of PSD of low frequency, PSD of high frequency are closer to the value of PSD from 7:39 to 8:04 frame. It has been modified, as follows:

Lines 653 to 656

The impact of flow velocity is more pronounced at the high-frequency end compared to the low-frequency end. This suggests that variations in flow velocity can be effectively discerned by analyzing the energy at the high-frequency end of the PSD curve.

C60: l.491-498: I think the figures are not appropriate to support your conclusions. In this passage, I don't understand how Figure 10 is related to what you say. I suggest you modify or add figure such that every statement in the article can be associated to a reference to a Figure, that illustrates clearly your point.

R60: We thank the reviewer for this comment. It is mistake of expression and translation. This part has been modified in the manuscript, as follows:

Lines 662 to 669

In the low-frequency range, velocity has a notable impact on energy. When velocity decreases, the energy corresponding to a single frequency also decreases, albeit with a relatively small amplitude compared to the high-frequency range, as illustrated in Fig. 9. Notably, there is an observable increase in the low-frequency end at 7:44 in contrast to 7:39, which contradicts the analysis of the high-frequency range. Fig. 7c displays an infrared image indicating a relatively high concentration of particles within the debris flow at 7:44. This observation suggests that the strong energy observed at the low-frequency end in this timeframe may be attributed to the presence of these particles.

C61: l.510-512: Following previous comments, I don't understand how you get to this conclusion.

R61: Thanks a lot for the constructive comment. We have modified the content and retranslated this part, which is shown in R3 for the general comments of reviewer 1 from lines 615 to 690.

C62: l.532-537: as stated above, you mention both frequency intervals and frequency values, such that it is not easy to understand your reasoning.

R62: Thank you for your constructive comments. This part mentioned by you has been modified, which is shown in R5 of general comment for reviewer 1 from lines 692 to 740.

C63: l.560 and following: How do you define the scale of a debris flow? Is it in terms of velocity? Discharge? Volume? This is not clear, as the result the comparison you carry out remains quite vague, and it is not clear how you get to the conclusion of paragraph 4.3. Besides, I would expect you to estimate the velocity using eq 8, why don't you do it?

R63: Thank you for the professional suggestion. This part is only semi-quantitative analysis. After consideration, we deleted Section 4.3 "debris flow scale analysis by seismic signal" because the part is not strongly convincing. Eq. (7) is a very ideal model. It needs to be used the integration form of the equation when debris flow near-field monitoring. The simplification of the integration is a non-linear equation. It is difficult to solve and can be used as a new research topic. Thus, we did not use Eq. (7) for evaluation.

C64: l.580 and following: You could estimate the uncertainty on cross-correlation result analysing the cross-correlation function. E.g., what is the time delays associated to the 10% highest values of the cross-correlation function? You could also compute cross correlations, and thus delays, on moving time windows. You would thus have an estimate of the evolution of the flow velocity. Finally, you compare velocities estimated with cross-correlations and Manning formula, but why don't you also compare the velocities estimated with eq 8?

R64: We deeply appreciate the reviewer carefully went through the manuscript line by line. Comiti et al. (2014) suggested that the cross-correlation function tends to underestimate debris flow velocity, which is the case here. A factor that might influence the velocity calculation based on the cross-correlation function is the distance between seismic sensors. The sensors deployed in this study are about 500 m

apart, and Arattano and Marchi (2005) suggested that spacing of 100+ m may reduce the accuracy of debris flow velocity calculation based on the cross-correlation function. This part above has been in Section 5.2, so we have not shown it in Section 4.3. The reason why we don't also compare the velocities estimated with Eq. (7) is shown as R63 for reviewer 1 above.

C65: l.595 – 609: All this should be in the Methodology section, not in the Results section.

R65: Thanks a lot for the helpful comment. As R24 for reviewer 1 shown in lines 322 to 346, we have changed sequence of this part, which has been moved to the Methodology section.

C66: l.605 : What is the wet perimeter?

R66: Thank you for the useful advice. χ can be used to estimate summation of bed length and lateral depth of the channel wetted by debris flow in the cross-section. The sentence above has been modified in Section 3.3. The definition of the wet perimeter is shown in Fig. 4.

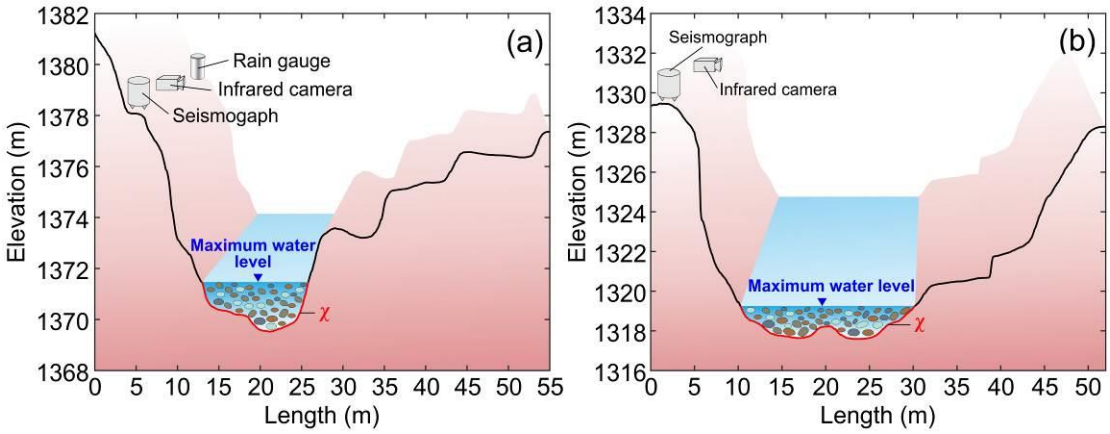

Fig. 4. Cross-sections of Fotangbagou gully showing maximum water level used in calculation of mean velocity by the Manning formula. (a) Monitoring station 1; (b) Monitoring station 2.

C67: l.611-612: You have a difference 11.29%, but the difference can come both from errors in the cross-correlation and from the Manning formula. Thus, it is not just an estimation of the error of the cross-correlation.

R67: We thank the reviewer for this helpful comment. Indeed, it is not appropriate to use 11.29% to explain an estimation of the error of the cross-correlation. Thus, the last sentence in Section 4.4 has been modified, as follows:

Lines 768 to 772

It indicates that the values of velocities are constant during process between the stations 1 and 2 because of the comparative wide and straight channel possibly. This indicates it is appropriate to use the cross-correlation function to estimate the velocity of debris flow because the two values from cross-correlation and from the Manning formula have a smaller difference.

C68: l.622-624: "Due to … relatively large", I don't understand this sentence, what do you mean? And how do you get to this conclusion?

R68: Thank you for spending the time to review and assess our manuscript. During the propagation of seismic in the crust, the energy of some seismic will be converted into thermal energy and lost. It is always called absorption attenuation. The magnitude of the absorption attenuation is positively related to extend of formation consolidation. However, debris flow monitoring site is usually located at the surface of earth and made up of loose deposit. It is the strongest absorption attenuation at this moment. The sentence has been modified, as follows:

Lines 778 to 781

Due to the strong absorption and attenuation during seismic waves traveling through the surface, the seismic signals especially for those recorded by the monitoring system in the vicinity of the channel often has a strong energy loss in high frequency.

C69: l.629-630: As said above, I would discuss if this frequency range can be related, or not, to the signal filtering that must be done prior to instrumental response deconvolution.

R69: Thank you so much for the comments. There is no instrument response document of seismograph. Thus, both signals of the two gullies cannot achieve instrument response. It will cause that logical sequence of signal of the two gullies exists difference. We will consider it mentioned by you in the subsequent research.

C70: l.638 – 640: "the debris flow must be … representative analysis point", I don't understand this sentence.

R70: We thank the reviewer for this comment. Because only several the PSD curve analysis time can be chosen, we should have a full consideration of the whole debris flow signal, which contributes to selecting more appropriate representative analysis points about seismic feature. This sentence has been modified in the manuscript, as follows:

Lines 797 to 798

When selecting the analysis time of PSD curve, it is necessary to fully consider the characteristics of debris flow seismic and select representative analysis points.

C71: l.660-662: Estimating the uncertainty and reliability of cross-correlation result as suggested before could help explain this high velocity.

R71: Thanks a lot for the constructive comment. Maybe our expression makes you misunderstand. Actually, we have explained it about the uncertainty and reliability of cross-correlation result. The uncertainty of the result owed to: "Comiti et al. (2014) suggested that the cross-correlation function tends to underestimate debris flow velocity, which is the case here. A factor that might influence the velocity calculation based on the cross-correlation function is the distance between seismic sensors. The sensors deployed in this study are about 500 m apart, and Arattano and Marchi (2005) suggested that spacing of 100+ m may reduce the accuracy of debris flow velocity calculation based on the cross-correlation function." It is in Section 5.2. The reliability of the result owed to: "This indicates it is appropriate to use the cross-correlation function to estimate velocity of debris flow because the two values from cross-correlation and from the Manning formula have a smaller difference." It is shown in R67 from lines 768 to 772, which has been modified in the last sentence of Section 4.3.

C72: l.686 "the 5 min interval … is fine for determining debris flow movement", I don't really agree, because I don't see how you can quantify the dynamics from one picture.

R72: Thank you for your constructive comments. Our study gullies don't usually have electric power and the instruments need battery to offer electric power which is lacking in the uninhabited area. The two gullies are lack of sunlight in complex mountainous areas and solar energy cannot be offered to ensure monitoring devices working normally. Thus, we use infrared cameras with 5-min interval shoots characterized by less power consumption instead of video equipment. After changing the structure of the manuscript, we achieved semi-quantitative analysis instead of quantitative analysis.

C73: You present in the abstract your method as general framework for debris flow monitoring. This is not apparent in the conclusion, where you mainly summarize the characteristics of the studied debris flow. You should highlight how your method can be applied to other sites, and what results are new in comparison to previous studies.

R73: Thank you for your professional suggestion. In this study, we take the 2nd Fotangbagou gully debris flow as an example to discuss the feasibility of our methodology and research ideas after the two other debris flows are relatively lack of information, at the same time like the 2nd Fotangbagou gully debris flow and then analyze the two other debris flows, the manuscript will also appear redundant. This study mainly uses seismic signals to analyze the whole evolution process of debris flows. We proposed a low-cost, reliable, convenient method to monitor debris flow based on seismic signal. Our research purpose is to solve the problem of difficulty in monitoring debris flow in complex mountainous areas, where lack of sunlight cannot offer solar energy to ensure monitoring devices working normally.

C74: l.705-706: The rapid increase / slow decay of seismic energy is expected, I don't think this is a major contribution of your work to the debris flow research field.

R74: We deeply appreciate the reviewer carefully went through the manuscript. We changed expression of the sentence. It has been modified, as follows:

Lines 875 to 876

Three debris flows were analyzed that they exhibit the seismic characteristics of fast excitation and slow recession.

C75: The quality of figures is not very good when they are printed, you should use higher dpi (but this is maybe caused by the exportation to pdf).

R75: Thanks a lot for the helpful comment. Some of figures don't have a good quality, so we have modified and reprinted figures to improve their quality.

C76: Table 1: For the seismographs and geophones, you should include the corner frequencies.

R76: Thank you for the useful advice. The seismographs and geophones don't have corner frequencies. The geophones have eigenfrequency of 4.5–150 Hz, which is used to explain range of accurate recording. The eigenfrequency can be considered as corner frequencies because they have a strongly similar definition. It has been modified, as follows:

Table 1 Instrument parameters for monitoring stations in the two study catchments.

Equipment	Instrument parameters	
	Fotangbagou gully	Ergou gully
Seismograph	Sampling rate 100 Hz Coner frequency not offered	—

Geophone	—	Sampling rate 100 Hz Coner frequency of 4.5–150 Hz
Rain gauge	Record once per hour with a resolution of 0.2 mm	
Infrared camera	1 shot every 5 minutes at 2592×1944, 1920×1080 dpi resolution during the day and at night	

C77: Table 2: Specify that the beginning and end time are determined from the seismic signals of one sensor (which one?), but that it does not necessarily corresponds the beginning and end time of the event (it was initiated above the stations and keeps propagating downstream).

R77: We thank the reviewer for this helpful comment. We have specified the beginning and end time of the three debris flows, which comes from the first monitoring station of Fotangbagou and the second monitoring station of Ergou. It has been reexplained. The starting and ending time are time when debris flow starts to pass by and didn't pass by at all. It has been modified, as follows:

Table 2 Starting and ending time of three debris flow events at Wenchuan, China (August 19, 2022), picked from the seismic signals. (The starting and ending time are time when debris flow starts to pass by and didn't pass by at all.)

	Fotangbagou		Ergou
	1st	2nd	
Starting	03:07 am	7:25 am	2:44 am
Ending	05:26 am	11:24 am	4:49 am

C78: Table 3: Explain in the legend why there are no results for the Manning formula in two cases.

R78: Thank you for spending the time to review and assess our manuscript. Since the nighttime infrared images could not be used, *R* could only be determined for the second debris flow in the Fotangbagou gully, which took place in daylight. It has been modified, as follows:

Table 3 Results of mean velocity calculations for Fotangbagou gully and Ergou gully debris flows.

Debris flow	Mean velocity calculated using each method (m/s)	
	Cross-correlation function	Manning formula
First debris flow in Fotangbagou Gully	3.0	—
Second debris flow in Fotangbagou Gully	7.0	7.9
Debris flow in Ergou Gully	38.3	—

Notation: Since the nighttime infrared images could not be used, *R* could only be determined for the second debris flow in the Fotangbagou gully, which took place in daylight.

C79: Figure 1: You should simplify the legend, especially as some labels are repeated (e.g. Granite). Consider adding a topographic map. The insert (a) is small and the satellite imagery is visible behind, you should improve that. Explain in the legend what the yellow lines are.

R79: Thank you so much for the comments. We have changed size of subplot (a) and (b) to solve the problem mentioned by you in this figure. Two topographic maps were added in Figure 2. The subplot (c) has been deleted. It has been modified, as follows:

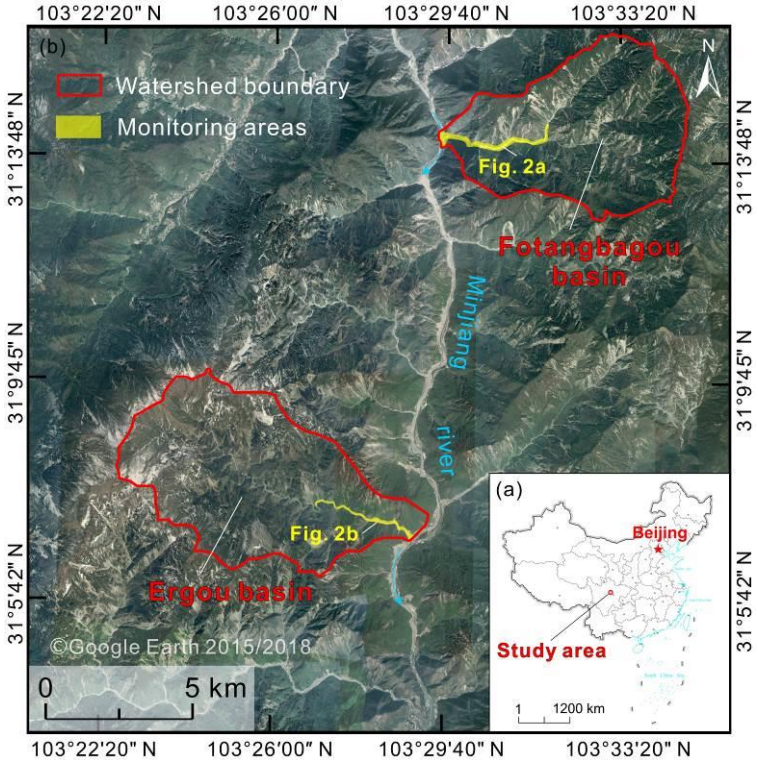

Fig. 1. Overview of the study area. (a) Location of the study area within China; (b) The two study catchments, Ergou and Fotangbagou, on the Minjiang River, Wenchuan, Sichuan, China.

C80: Figure 2: I'm not sure a picture of all stations is necessary. You should add a Digital Terrain Model map for the two gullies if you have one. A longitudinal profile could also be helpful.

R80: We thank the reviewer for this comment. We have added two Digital Terrain Model maps for the two gullies. It has been modified, as follows:

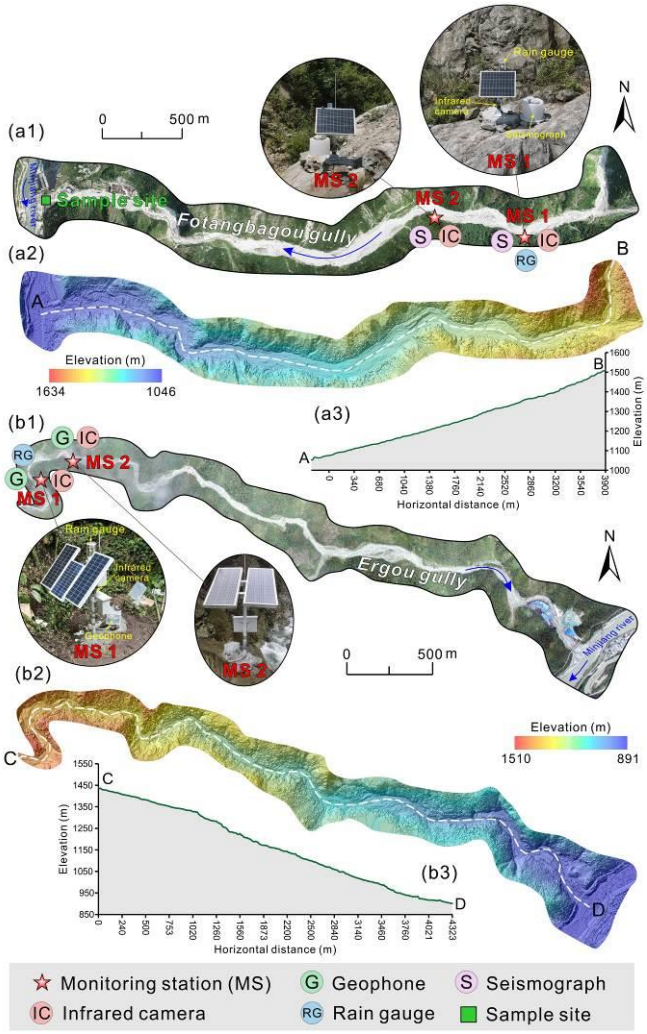

Fig. 2. Schematic overview of monitoring network layout in the two study catchments. (a) Fotangbagou gully: (a1) drone aerial photography, (a2) Digital Terrain Model map, (a3) longitudinal profile; (b) Ergou gully: (b1) drone aerial photography, (b2) Digital Terrain Model map, (b3) longitudinal profile. See Fig. 1 for gully locations.

C81: Figure 3: "Infrared imagery" only during the night! For "amplitude method" and "simplified signal", it is not clear what it corresponds to in the methodology presented in the main body of the article. Don't you estimate the maximum flow velocity from the seismic signal also? Be more specific when you mention "scale of the debris flow", do you mean discharge? Volume? See also the first specific comment for the Methodology section.

R81: Thanks a lot for the constructive comment. We can estimate the maximum flow velocity from the seismic signal. "Scale of the debris flow" has been deleted. It is not our research content. Amplitude method is used to get the absolute value of time-domain amplitude. After this method, the signal processed by us is called simplified signal. The two sentences have been added.

It has been modified to explain Fig. 3, as follows:

Lines 279 to 293

To extract information on debris flow evolution, debris flow seismic signals were processed and interpreted by following the procedure in Fig. 3. Absorption attenuation compensation is first to be processed for each frequency of the extracted seismic signal of debris flow to restore the different energy loss caused by different propagation, which was aimed to obtain the seismic signal of debris flow that is not affected by sensors installation location. Then, the seismic spectrogram is from compensated seismic signal based on short-time Fourier transform, characteristic analysis of debris flow evolution has been done by computing power spectral density of keyframe and the absolute value of time-domain amplitude, the evolution analysis result has been verified based on infrared imagery and post-event field investigation. Finally, the maximum velocity of debris flow has been estimated by computing the absolute seismic amplitude of different monitoring stations based on the cross-correlation function, which has been verified by the Manning formula. The key steps are outlined below in Fig. 3. Amplitude method in this figure is used to get the absolute value of time-domain amplitude in this figure. After this method, the signal processed by us is called a simplified signal.

The figure has been modified, as follows:

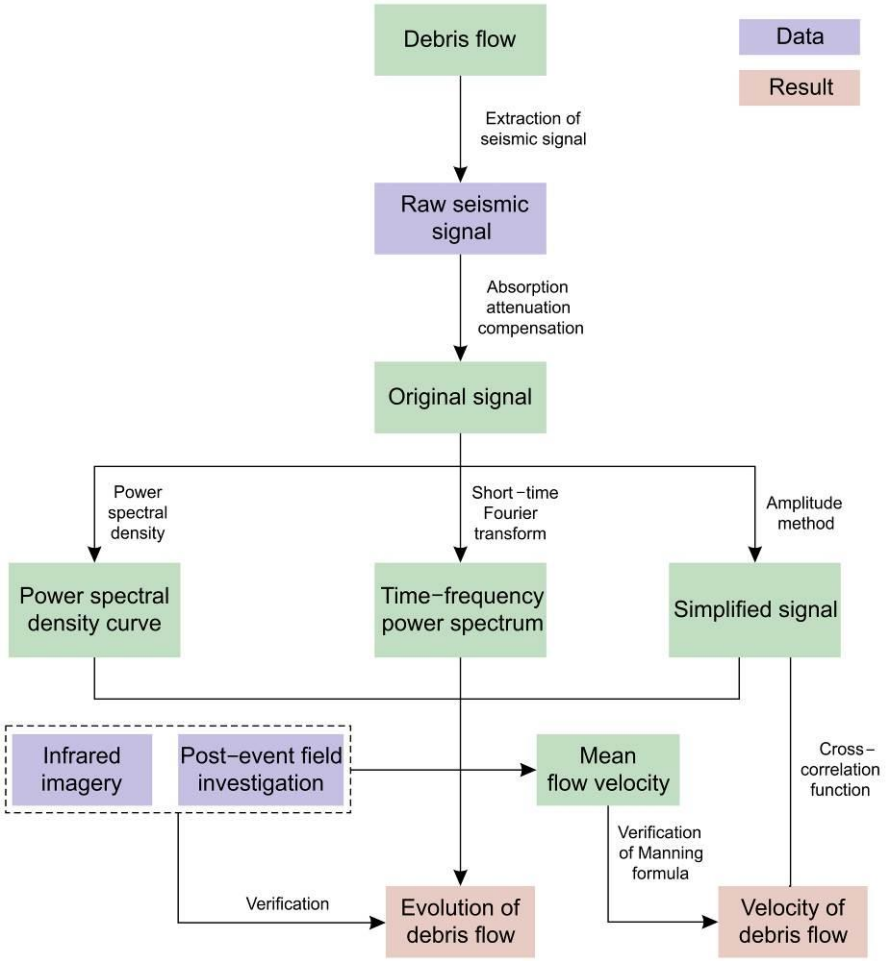

Fig. 3. Research methodology for processing and analysis of debris flow seismic signal.

C82: Figure 4: You should display the alleged start and end time of all three events to improve clarity. In a and c, the high amplitudes exceed the plot limit. Is it only a representation issue, or is the signal saturated? In the legend of (a), you say that there's only the second debris flow, but aren't there two?

R82: Thank you for your constructive comments. The alleged start and end time of all three events have been added in this figure. It is representation issue for the high amplitudes to exceed the plot limit. There is an error in the legend of (a), it has been modified into "raw seismic from Fotangbagou gully debris flow at station 1". It has been modified, as follows:

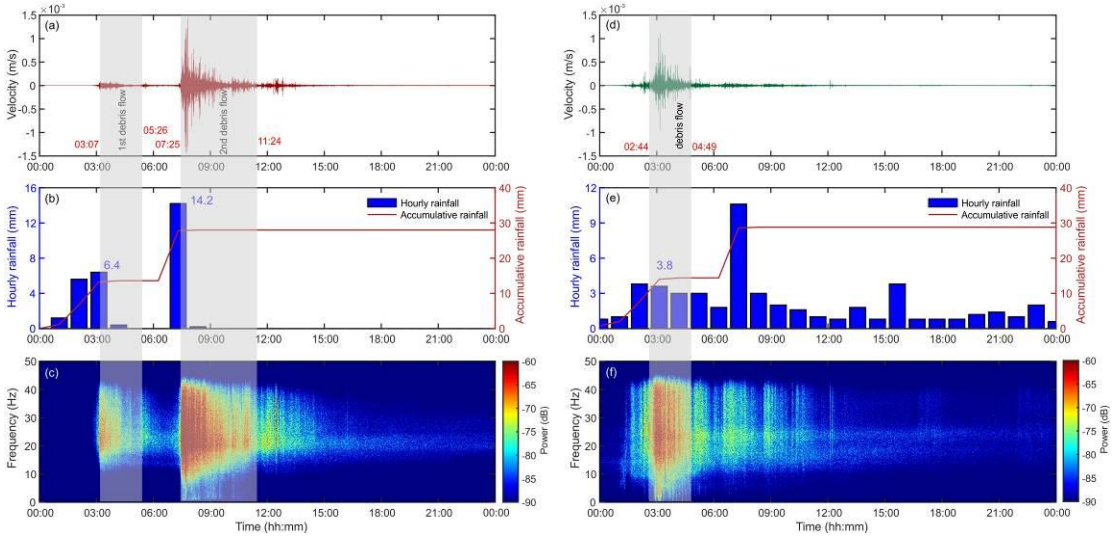

Fig. 5. Vertical seismic, rainfall and frequency spectrum of the debris flows. (a) Raw seismic from Fotangbagou gully debris flow at station 1; (b) rainfall at Fotangbagou gully; (c) spectrogram of (a) by STFT; (d) Raw seismic from Ergou gully at station 2; (e) rainfall at Ergou gully; (f) spectrogram of (d).

C83: Figure 5: You could add the seismic signals in the background, or at least the beginning and end time of all three events. The link with the precipitations would be more apparent.

R83: We totally agree with the reviewer's suggestion**.** This figure has been combined with Figure 4 in the first version. The beginning and end time of all three events have been added in the figure.

C84: Figure 6 and 7: Figure 7 use elements already present in Figure 6. Thus I would only display the damping factor and PSD in Figure 6. The "simplified signal" could also be displayed in Figure 7a and 7b. In the legend of Figure 6d, I think it is station 1, not station 2.

R84: Thank you for your professional comment. Figure 7 in the first version has been deleted because this figure has appeared in Figure 6 in the first version. In the legend of Figure 6d, it is station 1, it has been modified into "Time-frequency domain energy spectrum for monitoring station 1". It has been modified, as follows:

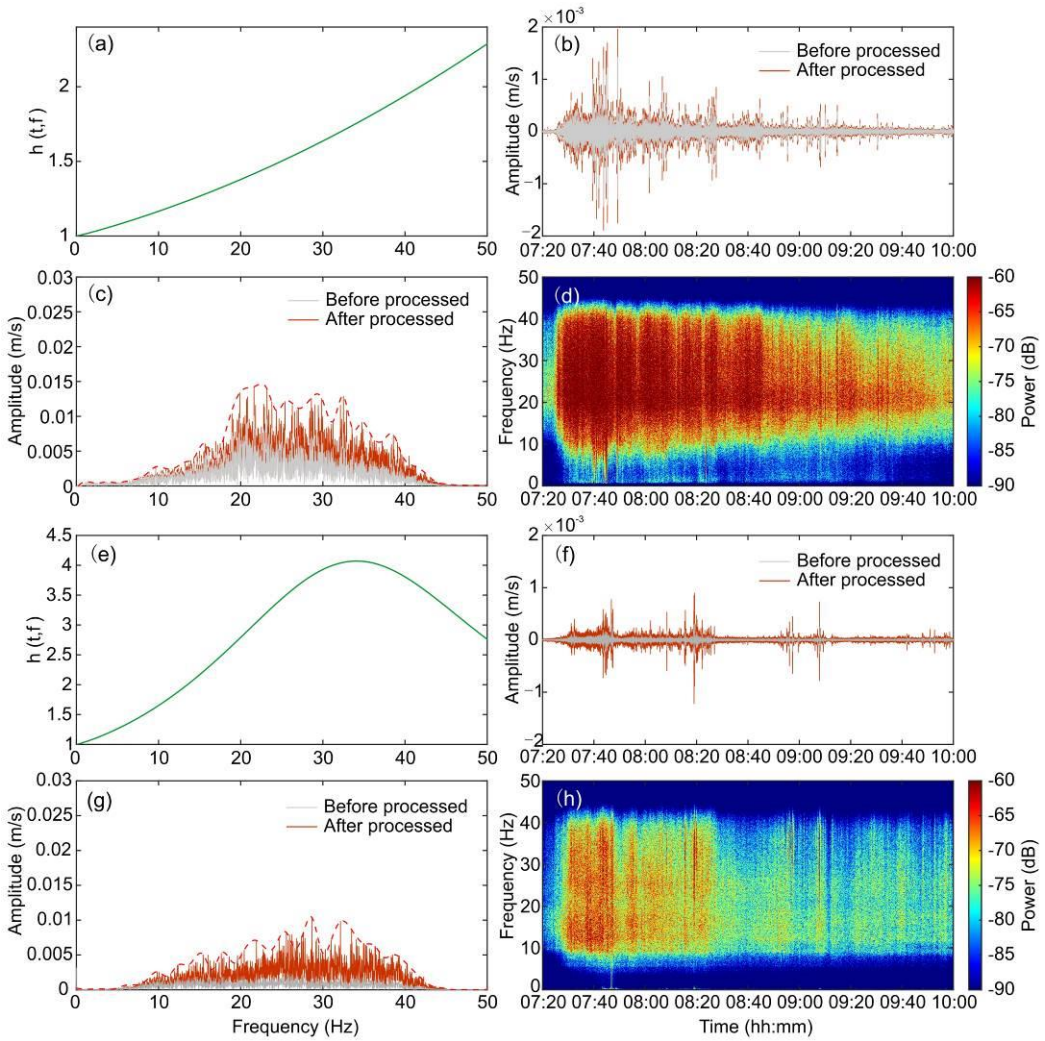

Fig. 6. Restored seismic signal for the second debris flow in Fotangbagou gully. (a) Compensation function curve for monitoring station 1; (b) Time domain signal at monitoring station 1; (c) Frequency domain signal at monitoring station 1; (d) Restored spectrogram for monitoring station 1; (e) Compensation function curve for monitoring station 2; (f) Time domain signal at monitoring station 2; (g) Frequency domain signal at monitoring station 2; (h) Restored spectrogram for monitoring station 2. The red dashed lines in (c) and (g) are envelopes that represent peak amplitudes after processing.

C85: Figure 8: Picture are very small, it is difficult to see the different behaviours of the debris flow at each time.

R85: Thanks a lot for the constructive comment. Pictures have been arranged to improve their clarity. It has been modified, as follows:

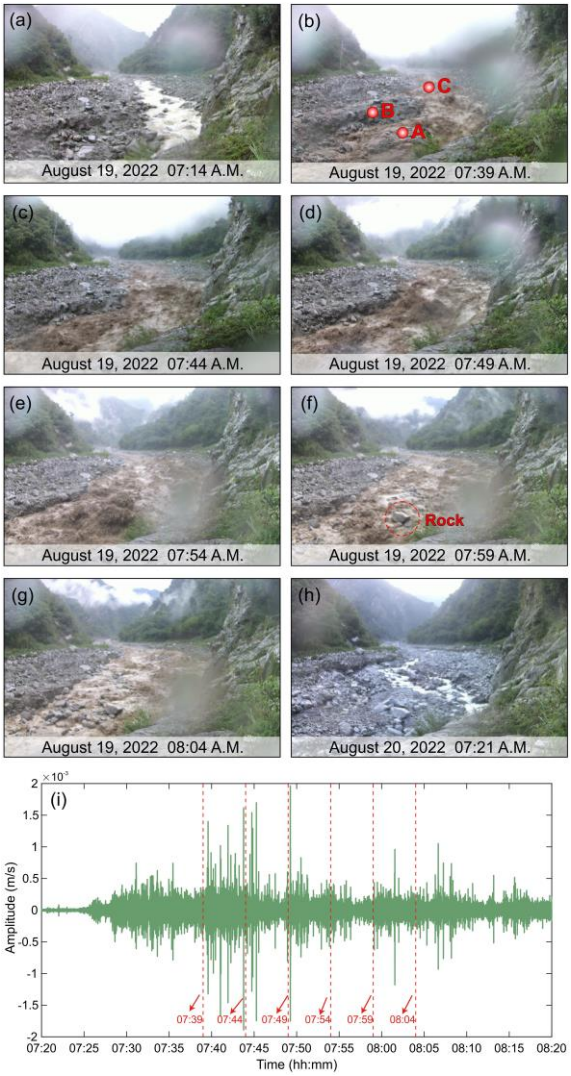

Fig. 7. Infrared camera images and seismic signals were recorded at monitoring point 1 in Fotangbagou Gully during the second debris flow on the morning of August 19, 2022. Images (b)-(g) were recorded every 5 minutes from 7:39 to 8:04: (a) before debris flow; (b) 7:39 frame; (c) 7:44 frame; (d) 7:49 frame; (e) 7:54 frame; (f) 7:59 frame; (g) 8:04 frame; (h) after debris flow. (i) The seismic signal was recorded at the point.

C86: Figure 9: "viscous particle" is not an appropriate term. In (d), you could add the granulometric ranges associated to gravel, sand, silt and clay.

R86: Thank you for the useful advice. "Viscous particle" has been modified into "clay". Range of gravel, sand, silt and clay has been added in subplot (d). It has been modified, as follows:

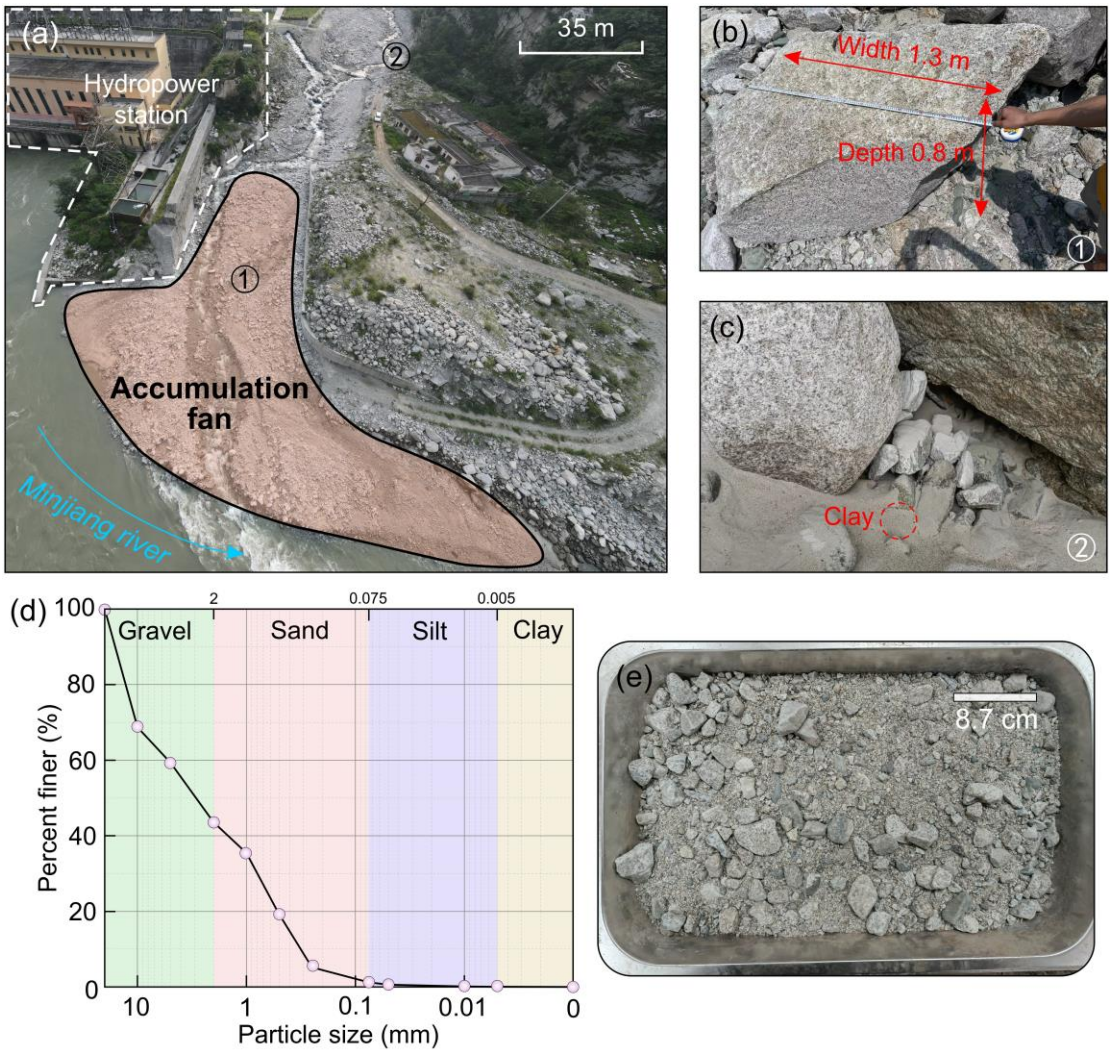

Fig. 8. Post-event field survey of accumulation fans in Fotangbagou Gully. (a) Aerial view of the Fotangbagou gully fan; (b) Largest particle on the Fotangbagou gully fan, marked ① in image (a); (c) Thin layer of clay covering the accumulation surface in Fotangbagou gully, marked as ② in image (a); (d) Particle size distribution for Fotangbagou gully sediment samples; (e) Fotangbagou gully sediment sample. Clay has not been marked in the subplot (d) because of the particles with grain size less than 0.005 mm.

C87: Figure 10: This plot is not easy to interpret. It must be improved / changed to better illustrate and support the statements made in the main body of the article. L.463 you mention "PSD maximum", it is not clear what this maximum corresponds to (maximum over what?).

R87: We thank the reviewer for this helpful comment. This figure has been divided into two figures. It would make the figures easy to interpret. It has been modified, as follows:

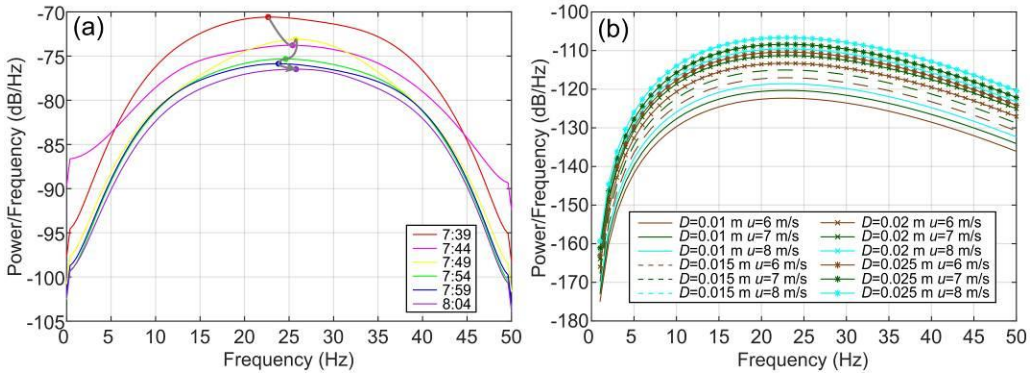

Fig. 9. Characteristic change of power spectral density (PSD). (a) Evolution of PSD during the second debris flow in Fotangbagou Gully on the morning of August 19, 2022, from 7:39 to 8:04; (b) Comparison of PSD for different grain sizes (D) and velocities (u). Each curve represents PSD frequency over 60 s. The six dots in subplot (a) correspond to the PSD maximum at the six-time points from 7:39 to 8:04, and the black arrows indicate the time course of these six-time points. The PSD values of D=0.015 m and u=8 m/s, D=0.02 m and u=6 m/s are equal, so the curves coincide in subplot (b).

C88: Figure 12: I think you don't explain how the amplitude time series are computed, what does it correspond to?

R88: Thank you for spending the time to review the figure. A sentence has been added to explain what you mentioned. It has been modified, as follows:

Lines 747 to 748

The signal lag time τ in Eq. (4) reflected by the peak amplitude of the second debris flow in Fotangbagou gully is 74 s (Fig. 11).

C89: Figure 13: This figure should be in the Methodology section, and should be improved to illustrate how the different parameters of the Manning formula are computed.

R89: Thank you so much for the comments.This figure has been moved to the Methodology section and added illustration of wet perimeter χ. It has been modified, as follows:

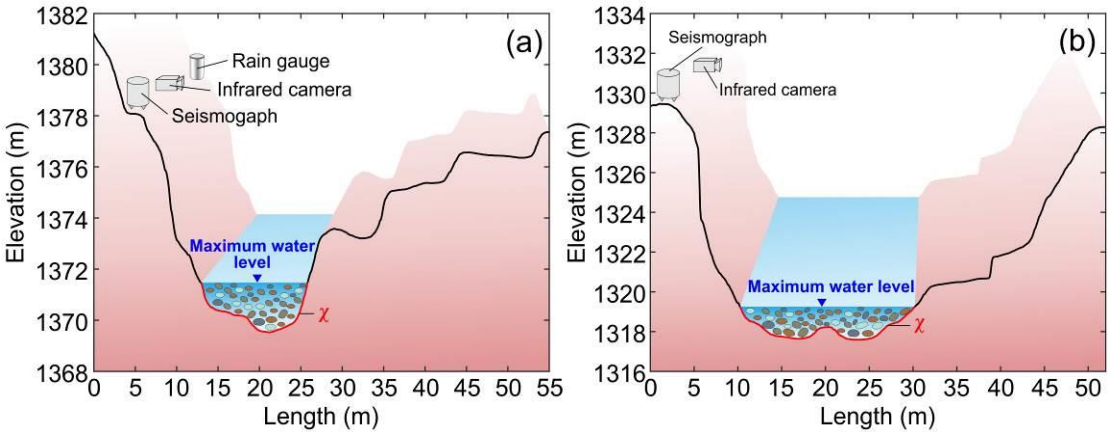

Fig. 4. Cross-sections of Fotangbagou gully showing maximum water level used in calculation of mean velocity by the Manning formula. (a) Monitoring station 1; (b) Monitoring station 2.

C90: l.27: The most important → an important.

R90: We thank the reviewer for this comment. It has been modified, as follows:

Lines 27 to 28

An important approach to mitigating debris flows is monitoring and early warning.

C91: l.31-32: debris flow imagery → be more specific, what do you mean by imagery?

R91: Thanks a lot for the constructive comment. "Debris flow imagery" means "debris flow monitoring images". It has been modified, as follows:

Lines 37 to 39

We comprehensively analyzed seismic signals and infrared images gained by the system with other post-event field investigations to obtain basic parameters such as debris flow velocity and grain size.

C92: l.34: basic parameters → be more specific, what parameters?

R92: Thank you for your constructive comments. "Basic parameters" means basic parameters (e.g., velocity, grain size and so on). It has been modified, which is shown in R91 from lines 37 to 39 for the specific comments of reviewer 1.

C93: l.39: Remove "and restore … as far as possible". You do not recover the unchanged signal because you do not correct for site effect. So I would just say that you correct for attenuation.

R93: We totally agree with the reviewer's suggestion. It has been modified, as follows:

Lines 39 to 42

First, we selected the second debris flow in the Fotangbagou gully as a case to show the process to determine the duration of the debris flow that passed the monitoring station by the energy recovered seismic signal, and establish that rainfall triggered the debris flow.

C94: l.41: "test rain" → what do you mean?

R94: Thank you for professional comment. There is an error during typing. Actually, it is not "test rain" but "rain". The word "test" has been removed in the manuscript.

C95: l.49: The cross-correlation is not an algorithm. What do you mean by "verifying Manning's formula"?

R95: Thanks a lot for the constructive comment. The word "algorithm" has been removed. There is an error in "verifying Manning's formula", which should be modified into "confirmed by the Manning's formula". It has been modified, as follows:

Lines 47 to 49

Finally, the cross-correlation function is used to calculate the maximum velocity of 7.0 m/s of the second debris flow, which was confirmed by the Manning formula.

C96: l.61: "huge" → "massive". Quantify your statement in terms of velocity / discharge.

R96: Thank you for the useful advice. It has been modified, as follows:

Lines 62 to 64

Debris flows unlike landslides comprise a solid-fluid mixture that, under heavy rainfall (Iverson, 1997), can generate massive surges that cause damage and loss of life.

C97: l.67-68 "with monitoring … at present". I don't understand this sentence.

R97: We thank the reviewer for this helpful comment. This sentence aims to explain "disaster reduction measures" ahead in detail. It has been modified, as follows:

Lines 68 to 71

Given the significant hazard potential of debris flows, there is considerable interest in disaster reduction measures, particularly in instruments based on seismic and flow depth monitoring. Currently, the most widely used approaches are monitoring and early warning systems.

C98: l.75: "on different aspects", this is vague, be more specific or remove.

R98: Thank you for the useful advice. The words "different aspects of" has been removed in manuscript.

C99: l.87: "evolutionary characteristics", which ones?

R99: Thank you so much for the comments. "Evolutionary characteristics" means parameters such as grain size in debris flow and so on. It has been modified, as follows:

Line 90 to 92

Flow depth and velocity are usually combined with monitoring section geometry to estimate discharge and analyze evolutionary characteristics like grain size of debris flows and so on (Arattano and Marchi, 2008; Hürlimann et al., 2019).

Reference

Hürlimann, M., Coviello, V., Bel, C., Guo, X., Berti, M., Graf, C., Hürl, J., Miyata, S., Smith, J.B., Yin, H.-Y., 2019. Debris-flow monitoring and warning: Review and examples. Earth-Sci. Rev. 199, 102981.

C100: l.96: It's not monitoring and early warning-systems that must identify potential sites. Instead, potential sites must be evaluated for the development of monitoring and early-warning systems

R100: We thank the reviewer for this comment. It has been modified, as follows:

Lines 103 to 105

It is essential to assess potential sites in advance for the deployment of monitoring and early-warning systems, ensuring that suitable instrumentation can be installed.

C101: l.98 “close-range monitoring instruments”: be more precise, which ones?

R101: Thanks a lot for the constructive comment. “Close-range monitoring instruments” contains rain gauge, velocity instrument and so on. It has been modified, as follows:

Lines 117 to 120

However, the abruptness of onset and high strength of the initial debris flow surge often damage close-range monitoring instruments like rain gauge, velocity instrument and so on making it difficult to obtain a complete dataset of the entire debris flow process.

C102: l.115: “a new physical debris flow model”, I think “new methodology” or “approach” is more appropriate. A debris flow physical model refers to an experiment at the laboratory scale.

R102: Thank you for your constructive comments. It has been modified, as follows:

Lines 147 to 149

Lai et al. (2018) proposed a new methodology that allows flow velocity and distance to be calculated based on the amplitude and frequency characteristics of the seismic signal.

Reference

Lai, V.H., Tsai, V.C., Lamb, M.P., Ulizio, T.P., Beer, A.R., 2018. The seismic signature of debris flows: Flow mechanics and early warning at Montecito, California. Geophys. Res. Lett. 45(11), 5528-5535.

C103: l.123 “identification” → detection

R103: We totally agree with the reviewer’s suggestion. It has been modified, as follows:

Lines 157 to 162

Current research on seismic monitoring and debris-flow early warning concentrates on event timing (Walter et al., 2017; Huang et al., 2020; Beason et al., 2021), location (Walter et al., 2017; Lai et al. al., 2018), evolution of parameters such as velocity and discharge (Arattano, 1999; Lai et al., 2018; Andrade et al. 2022; Schimmel et al., 2022), and detection (Bessason et al., 2007; Schimmel and Hübl, 2016; Huang et al., 2020).

Reference

Andrade, S.D., Almeida, S., Saltos, E., Pacheco, D., Hernandez, S., Acero, W., 2022. A simple and general methodology to calibrate seismic instruments for debris flow quantification: application to Cotopaxi and Tungurahua volcanoes (Ecuador). Landslides 19(3), 747-759.

Arattano, M., 1999. On the use of seismic detectors as monitoring and warning systems for debris flows. Nat. Hazards 20(2-3), 197-213.

Beason, S.R., Legg, N.T., Kenyon, T.R., Jost, R.P., 2021. Forecasting and seismic detection of proglacial debris flows at Mount Rainier National Park, Washington, USA. Environ. Eng. Geosci. 27(1), 57-72.

Bessason, B., Eiríksson, G., Thorarinsson, Ó., Thórarinsson, A., Einarsson, S., 2007. Automatic detection of avalanches and debris flows by seismic methods. J. Glaciol. 53(182), 461-472.

Huang, X., Li, Z., Fan, J., Yu, D., Xu, Q., 2020. Frequency characteristics and numerical computation of seismic records generated by a giant debris flow in Zhouqu, Western China. Pure Appl. Geophys. 177, 347-358.

Lai, V.H., Tsai, V.C., Lamb, M.P., Ulizio, T.P., Beer, A.R., 2018. The seismic signature of debris flows: Flow mechanics and early warning at Montecito, California. Geophys. Res. Lett. 45(11), 5528-5535.

Schimmel, A., Coviello, V., Comiti, F., 2022. Debris flow velocity and volume estimations based on seismic data. Nat. Hazards Earth Syst. Sci. 22(6), 1955-1968.

Schimmel, A., Hübl, J., 2016. Automatic detection of debris flows and debris floods based on a combination of infrasound and seismic signals. Landslides 13, 1181-1196.

Walter, F., Burtin, A., McArdell, B.W., Hovius, N., Weder, B., Turowski, J.M., 2017. Testing seismic amplitude source location for fast debris-flow detection at Illgraben, Switzerland. Nat. Hazards Earth Syst. Sci. 17(6), 939-955.

C104: l.131-134: Make two sentences to improve clarity.

R104: Thank you for the useful advice. This paragraph where the sentences are located has been modified, as follows:

Lines 172 to 182

As for characteristics of debris flow in the western part of China, we designed a near-field debris flow monitoring system, which is comprised of seismic equipment, rainfall gauge, and infrared camera, and monitored three debris flows on August 19, 2022, in the Wenchuan Earthquake area of China. Then, we do a comprehensive analysis of recovered seismic data, infrared imagery, post-event field investigation,

and rainfall data and gain semi-quantitative data on the debris flow. The study offers a framework for establishing debris flow monitoring and semi-quantitative analysis based on seismic signals. It introduces a cost-effective, dependable, and convenient approach for monitoring debris flows in intricate mountainous terrains, where insufficient sunlight impedes the normal functioning of solar-powered monitoring equipment.

C105: l.135: "theoretical basis". You did not develop a new theory, so this is not appropriate.

R105: Thanks a lot for the constructive comment. This paragraph where the sentences are located has been modified, which shown in R104 for reviewer 1.

C106: l.144 "steep gradients" → steep slope gradients.

R106: Thank you for the useful advice. It has been modified, as follows:

Lines 188 to 189

The area is typical of that formed by tectonic uplift and river erosion, with undulating terrain, ravines, and steep slope gradients.

C107: l.171: "adequate water sources", what do you mean by adequate?

R107: We thank the reviewer for this helpful comment. "Adequate" in "adequate water sources" means rich, abundant. It has been modified, as follows:

Lines 189 to 191

River channel gradients range from 5° to 30°, hillslopes range from 25° to 50°, and most of the area has a humid climate with annual abundant rainfall of 800-1200 mm (Guo et al., 2016).

C108: l.176: Station 2 is below station 1 but using "downstream" makes the reader believe it is at the outlet of the gully. So you should rephrase to avoid misinterpretation.

R108: Thank you for spending the time to review and assess it. It has been modified, as follows:

Lines 249 to 252

Monitoring systems comprising an array of instruments were set up at station 1 (3260 m from the mouth in Fotangbagou Gully and 4130 m in Ergou Gully) and 2

monitoring points along the current in the gullies (Table 1, Fig. 2), in 2022 and 2021 respectively.

C109: l.186-187: the distances from the outlet should be given at the beginning of the paragraph when you locate the stations, it would be more logical.

R109: Thank you so much for the comments. It has been modified which is shown in R108 for reviewer 1.

C110: l.209 eq 1: Explicit what X and x are. You should use the same conventions than for eq 7 and 4 : t or n for the time, X or S for the Fourier coefficient, omega or f for the angular frequency / signal frequency. You must use a different notation for the window function and the angular frequency, and explicit the notation of the window function

R110: We thank the reviewer for this comment. Firstly, X and x are signals of time-frequency, time domain, respectively Eq. (1). Secondly, n and t in Eq. (1) and 4, X or S in Eq. (4) and (7) have been modified into t, X for the same conventions. Because of satisfying relationship, $f=2\pi\omega$, ω and f have not used the same convention. Thirdly, a notation of window function has been modified into W in Eq. (1). Above all, it has been modified, as follows:

Lines 298 to 306

The short-time Fourier transform (STFT, Eq. (1)) is used to analyze the time-frequency domain characteristics of the debris flow seismic signal (Yan et al., 2021, 2022, 2023). The method allows the time domain and frequency domain characteristics of the signal to be analyzed simultaneously:

$$X(t, \omega) = \sum_{m=-\infty}^{\infty} x(m)W(t-m)e^{-j\omega m}, \qquad (1)$$

where X and x are signals of time-frequency and time domain, W is the window function, m is the start time of the window function, ω is the angular frequency, e is a natural constant, t is time, and j is the imaginary number (Yan et al., 2021). A Hanning window length of 2056 and a time length of 20.56 s correspondingly is used. A built-in function “spectrogram” of MATLAB is used to achieve STFT directly from the software manual.

C111: l.210: “window start time”, what window? You did not define it before.

R111: Thanks a lot for the constructive comment. It has been modified which is shown in R110 for reviewer 1.

C112: l.211 "n is the time series", this is not clear, the time series is x, not m. n is the central time of the window function, and m the varying time index.

R112: Thank you for your constructive comments. It has been modified which is shown in R108 for reviewer 1.

C113: l.212: "length of 2056", you should give the corresponding length in seconds.

R113: We totally agree with the reviewer's suggestion. It has been modified which is shown in R108 for reviewer 1.

C114: l.214-216: "Since the signal propagates to many places" → not clear, reformulate. Or you can simply delete the first sentence and start directly the paragraph with "The croos-correlation…", and introduce afterwards the definition of Phi with associated notations.

R114: We deeply appreciate the reviewer carefully went through the manuscript line by line. The first sentence has been deleted. "ϕ" is used to represent sign of cross-correlation function as a notation. Above all, it has been modified, as follows:

Lines 308 to 312

The cross-correlation function is used to compute the time delay of τ that corresponds to the travel duration of the source between the stations. The time delay of the signals comes from sampling signals, such as M signal samples $[x_K]$, $[y_K]$ in Eq. (2) and (3) at different locations when the maximum calculation result $\phi_{yx}(\tau)$ is obtained based on Eq. (4) (Arattano and Marchi, 2005).

C115: l.216: The cross-correlation is not an algorithm, it's just a mathematical function.

R115: Thanks a lot for the constructive comment. "Cross-correlation algorithm" has been modified into "cross-correlation function" in the whole manuscript. It has been modified, as follows:

Lines 308 to 309

The cross-correlation function is used to compute the time delay of τ that corresponds to the travel duration of the source between the stations.

C116: l.222 eq 4: the equation is not well defined for the last values of t, as t+tau can be superior to M-1 and y is not defined in this case.

R116: Thank you for the useful advice. When t exceeds M-τ-1 and is less than 0, $x_t y_{t+\tau}$ is equal to 0. y from station 2 is another signal of time domain for the same event as x from station 1. It has been modified, as follows:

Lines 318 to 320

$$\left[x_K\right]=\left[x_0, x_1, x_2, \ldots, x_{M-1}\right] \tag{2}$$

$$\left[y_K\right]=\left[y_0, y_1, y_2, \ldots, y_{M-1}\right] \tag{3}$$

$$\phi_{yx}(\tau)=\sum_{t=0}^{M-1} x_t y_{t+\tau}\ , \tag{4}$$

where y from station 2 is another signal of time domain for the same event as x from station 1, t and K which are absolute sampling time series from 0 to M-1, ϕ represent cross-correlation function. When t exceeds M-τ-1 and is less than 0, $x_t y_{t+\tau}$ is equal to 0.

C117: l.223: K is not defined.

R117: We thank the reviewer for this helpful comment. K is absolute sampling time series, which is shown in R116 for reviewer 1.

C118: l.238 eq 7: You combine the sum notation with the capital sigma, and the integral notation with df. Choose one.

R118: Thank you for spending the time to review and assess it. The equation has been removed df. It has been modified, as follows:

$$PSD_{f_{\min}\sim f_{\max}}(t)=\frac{1}{(f_{\max}-f_{\min})}\times\sum_{f=f_{\min}}^{f_{\max}} X(t, f)\,, \tag{6}$$

C119: l.243: Define what the effective length L is.

R119: Thank you so much for the comments. It has been modified, as follows:

Lines 362 to 363

L is effective length of L=r_0.

C120: l.249: "Elastic wave travel through the earth is energy dissipation and velocity dispersion", this sentence must be clarified.

R120: We thank the reviewer for this comment. It has been modified, as follows:

Line 379

Elastic wave travel makes energy and velocity smaller.

C121: l.286: "the eruption" → the onset.

R121: Thanks a lot for the constructive comment. It has been modified, as follows:

Lines 432 to 434

The analysis of rainfall data indicates the presence of precipitation preceding the onset of the three debris flows. Furthermore, the rainfall data can be examined in terms of its initiation time and the time of significant amplitude changes in seismic signals.

C122: l.298-301: "Plane waves … by debris flow" : Rephrase these two sentences, they are not clear.

R122: Thank you for your constructive comments. The two sentences have been modified, as follows:

Lines 442 to 445

When plane waves propagate through the subsurface of the Earth, they exhibit varying levels of dissipation with frequency, as expressed in Eq. (8). To mitigate some of the losses and enhance the fidelity of the seismic signals triggered by debris flow, we employ Eq. (9) to recovery the energy loss with different frequency.

C123: l.338: "reflection", the term is not appropriate

R123: We totally agree with the reviewer's suggestion. It has been modified, as follows:

Lines 471 to 473

To obtain the embodiment of debris flow evolution on seismic signals, we first processed the seismic signals according to the process shown in Fig. 2 and got the time- and time-frequency figures (Fig. 6).

C124: l.420 and following : instead of talking of "cohesive materials", you should use the standard classes of granulometry (gravel, sand, silts, clays).

R124: Thank you for the professional comment. It has been modified, as follows:

Lines 580 to 582

Field measurements indicate the fan is about 1.2 m thick, with a thin layer (1–2 mm) of clay covering the surface in several areas (Fig. 8c).

C125: l.421: "huge rocks", they are not that huge.

R125: Thanks a lot for the constructive comment. "huge" has been removed in the manuscript.

C126: l.565: "the comparison of the amplitude will be increased", what do you mean?

R126: Thank you for the professional advice. This section where the sentence is located has been deleted after we change the structure of the manuscript, so the sentence was also deleted.

C127: l.679 "experientially" → experimentally?

R127: We thank the reviewer for this constructive comment. This sentence has been deleted because it is about the scale analysis.

C128: l.689 "increased" → decreased.

R128: Thank you for spending the time to review and assess it. It has been modified, as follows:

Lines 859 to 860

In follow-up studies, the interval between images should be decreased.

C129: l.721-723: "the second debris flow … Manning formula", this sentence is not very clear, you should reformulate.

R129: Thank you so much for the comments. It has been modified, as follows:

Lines 890 to 892

Compared with the result based on the Manning formula, it is reasonable for calculation result of the mean velocity of 7.0 m/s for the second debris flow in Fotangbagou gully.